Journal of Geophysical Research: Solid Earth

RESEARCH ARTICLE
10.1002/2017JB014890

Probabilistic Hazard From Pyroclastic Density Currents in the Neapolitan Area (Southern Italy)

Laura Sandri[1], **Pablo Tierz**[1,2], **Antonio Costa**[1], **and Warner Marzocchi**[3]

[1]Istituto Nazionale di Geofisica e Vulcanologia, Sezione di Bologna, Bologna, Italy, [2]British Geological Survey, The Lyell Centre, Edinburgh, UK, [3]Istituto Nazionale di Geofisica e Vulcanologia, Sezione di Roma 1, Rome, Italy

Key Points:
- We compute a novel multivolcano probabilistic hazard assessment for PDC invasion at Napoli (Italy), in the next 50 years
- The hazard assessment provides a comprehensive quantification of aleatory and epistemic uncertainty
- We present an ensemble model to account for the unknown distribution of column collapse height

Supporting Information:
- Supporting Information S1
- Data Set S1

Correspondence to:
L. Sandri,
laura.sandri@ingv.it

Citation:
Sandri, L., Tierz, P., Costa, A., & Marzocchi, W. (2018). Probabilistic hazard from pyroclastic density currents in the Neapolitan area (Southern Italy). *Journal of Geophysical Research: Solid Earth*, *123*. https://doi.org/10.1002/2017JB014890

Received 18 AUG 2017
Accepted 30 MAR 2018
Accepted article online 6 APR 2018

Abstract The metropolitan area of Napoli (~3 M inhabitants) in southern Italy is located in between two explosive active volcanoes: Somma-Vesuvius and Campi Flegrei. Pyroclastic density currents (PDCs) from these volcanoes may reach the city center, as witnessed by the Late Quaternary stratigraphic record. Here we compute a novel multivolcano Probabilistic Volcanic Hazard Assessment of PDCs, in the next 50 years, by combining the probability of PDC invasion from each volcano (assuming that they erupt independently) over the city of Napoli and its surroundings. We model PDC invasion with the energy cone model accounting for flows of very different (but realistic) mobility and use the Bayesian Event Tree for Volcanic Hazard to incorporate other volcano-specific information such as the probability of eruption or the spatial variability in vent opening probability. Worthy of note, the method provides a complete description of Probabilistic Volcanic Hazard Assessment, that is, it yields percentile maps displaying the epistemic uncertainty associated with our best (aleatory) hazard estimation. Since the probability density functions of the model parameters of the energy cone are unknown, we propose an ensemble of different hazard assessments based on different assumptions on such probability density functions. The ensemble merges two plausible distributions for the collapse height, reflecting a source of epistemic (specifically, parametric) uncertainty. We also apply a novel quantification for a spatially varying epistemic uncertainty associated to PDC simulations.

1. Introduction

Pyroclastic density currents (PDCs) are ground-hugging mixtures of gases and pyroclasts commonly traveling at few to tens of m/s and reaching temperatures in the order of hundreds of °C (e.g., Branney & Kokelaar, 2002; Valentine, 1998). Together with lahars, PDCs have been the volcanic phenomenon responsible for the highest death toll in the last four centuries (Auker et al., 2013) and are among the causes of major concern in volcanic emergency management, as the most safe action to protect population against PDCs is the call for evacuations, sometimes on a large scale (e.g., Marzocchi & Woo, 2009).

The generation, transport, and deposition of PDCs are governed by a chain of very complex processes, which have long attracted the attention of scientists as a challenging problem to be modeled. A whole range of different simulators have been proposed, from very simple ones like the Energy Line (or energy cone in 3D, Malin & Sheridan, 1982) to more detailed numerical models considering friction within the flow and between the flow and the underlying ground (e.g., Titan2D and VolcFlow, see respectively Kelfoun & Druitt, 2005; Patra et al., 2005) and up to very complex fluid dynamical models that are able to consider the multiphase and multicomponent nature of PDCs (e.g., Esposti Ongaro et al., 2008).

So far, the use of PDC simulators has been mostly twofold: on one hand, they have been used retrospectively to reconstruct the dynamics (and related variables) of some past eruptions, by best fitting direct observations (e.g., Clarke et al., 2002; Ogburn et al., 2014) or some specific features of their PDCs deposits (e.g., Charbonnier & Gertisser, 2012; Dellino et al., 2008); on the other hand, they have been used prospectively to model the hazard posed by PDCs at a given volcano (e.g., Oramas-Dorta et al., 2012; Sheridan et al., 2004). Although complex models have been increasingly used in both cases, their use is often implicitly based on the questionable logic "the more details, the better" (Salt, 2008). In general, a model has to be judged only on its capability to describe one or more variables of interest, and not in terms of its complexity. Indeed, in modeling the hazard posed by complex processes such as PDCs, a necessary balance must be reached between model complexity (the more complex the simulator, the higher its computational cost) and the possibility to quantify uncertainty by fully

exploring the model parameters' space. The physical complexity of PDC-related processes implies that there are substantial uncertainties that cannot be neglected, stemming from the intrinsic natural variability of such processes (aleatory variability) and from our lack of knowledge or available data (epistemic uncertainty). In the specific case of Probabilistic Volcanic Hazard Assessment (PVHA), complex models cannot be currently run many times and thus they cannot explore and quantify uncertainty satisfactorily, hampering their capability to provide a complete and reliable PVHA.

A few recent works have tried to fully account for uncertainties in modeling the hazard posed by PDCs. In particular, Dalbey et al. (2008) applied the Titan2D model (coupled with Polynomial Chaos Quadrature) to produce probability maps, conditional upon the occurrence of PDCs within a given volume range, at Volcán de Colima (Mexico). Bayarri et al. (2009) and Spiller et al. (2014) developed a Bayesian emulator for the Titan2D simulator to produce hazard curves (Tonini, Sandri, Costa, et al., 2015) at a few locations around Soufriére Hills volcano in Montserrat. These hazard curves are conditional upon the occurrence of PDCs or applicable to a given time window. Nonetheless, the physical assumptions at the basis of Titan2D equations make it suitable only to simulate dense PDCs.

More recently, Neri et al. (2015) produced probability maps (mean and percentile maps, quantifying aleatory, and epistemic uncertainties) of PDC invasion in case of an inland explosive eruption from Campi Flegrei (Italy) by applying an integral model based on a modification of the box model by Huppert and Simpson (1980), and assuming the topography of the Campi Flegrei caldera as flat. As input to the model, the authors used a set of statistical distributions for the PDC invaded area during next eruption, which are built on past PDC deposits, in combination with expert elicitation techniques. Worthy of note, the modified box model used by Neri et al. (2015) only applies to dilute PDCs propagating over a subhorizontal surface. This hampers its use on volcanoes with predominant topographic structures, such as stratovolcanoes like Somma-Vesuvius, although the issue of the influence of topographic structures on dilute currents has been recently addressed by Ongaro Esposti et al. (2016). Further, the methodology adopted by Neri et al. (2015) requires the availability of a significant number of data on the areas invaded by past PDCs at the volcano of interest, and this favorable situation is not very common.

In order to explore the possibility of using the energy cone model to produce probability maps of areas invaded by PDCs, Tierz, Sandri, Costa, Sulpizio, et al. (2016) studied how aleatory and diverse sources of epistemic uncertainty influence the outputs of the energy cone (i.e., invaded area and maximum runout distance, two very relevant observables for PDC hazard) at Somma-Vesuvius, when

1. Running the energy cone on digital elevation models (DEMs) of varying horizontal resolution;
2. Using different probability distributions (reflecting different hypothesis on the flow generation and propagation) for the model parameters, that is, the eruption column collapse height H_0, and the flow mobility, usually parameterized by the ϕ angle (technically, the energy decay rate, expressed as the angle between the energy line and the horizontal): the smaller the ϕ angle, the slower the energy decay and thus the more mobile the flow (Malin & Sheridan, 1982);
3. Exploring diverse theoretical assumptions on the correlation patterns between the model parameters (independent, inverse or direct);
4. Quantifying, in a preliminary way, the intrinsic limitations of the energy cone model.

According to such a study, all the types of epistemic uncertainty explored affect significantly the final output of the energy cone model, in terms of invaded area and maximum runout. Furthermore, the largest contribution to epistemic uncertainty results from the so-called theoretical uncertainty (third item in the list above). Such correlation is controversial, as some studies (e.g., Doyle et al., 2010) support the idea of a direct correlation between collapse height and PDC mobility, while some others (e.g., Esposti Ongaro et al., 2008) suggest an inverse one.

Further, Tierz, Sandri, Costa, Zaccarelli, et al. (2016) implemented a quantitative procedure to test the performance of the energy cone at Somma-Vesuvius and Campi Flegrei, in the context of probabilistic volcanic hazard assessment. In particular, they blindly compared the invasion areas and maximum runouts measured from past PDC deposits at Somma-Vesuvius (Gurioli et al., 2010; Hazlett et al., 1991) and Campi Flegrei (Orsi et al., 2004) with those obtained from energy cone simulations. The term "blindly" implies that the data set used to set up the energy cone simulations was fully independent of the data set used to test the model performance, the latter consisting of real observations from PDC deposits from Somma-Vesuvius and

Campi Flegrei. In particular, Tierz, Sandri, Costa, Zaccarelli, et al. (2016) used independent data from eruption column simulations at Somma-Vesuvius and Campi Flegrei (after Sandri et al., 2016) and from worldwide data on PDC mobility (e.g., Hayashi & Self, 1992; Ogburn, 2012; Sheridan & Malin, 1983) to set up probability density functions for the model parameters (H_0 and ϕ).

The probability density functions set up for the ϕ angle (see section 2.2.2) cover a considerable range of values, spanning from low values typical of dilute PDCs (e.g., 4–11°; Sheridan & Malin, 1983), to larger values, more typical of dense PDCs. Then, by sampling the parameter space in a Monte Carlo scheme, Tierz, Sandri, Costa, Zaccarelli, et al. (2016) ran the energy cone model many thousands of times, obtaining the distributions of the simulated invaded area and maximum runout. The comparison with real (and, to the model, new) data from Somma-Vesuvius and Campi Flegrei has shown that observations are generally in statistical agreement (i.e., real data have p values larger than 1% of being exceeded with the simulator) with the set of energy cone simulations. In other words, despite being a simple model (e.g., Best et al., 2015), the energy cone model seems to capture the natural variability that an adequate hazard assessment should display.

Under these premises, in this paper, we apply the energy cone model to simulate the invasion of PDCs from Somma-Vesuvius and Campi Flegrei on the Napoli metropolitan area in Southern Italy where about 3 million people live. The results of the simulations are included in a Bayesian Event Tree for Volcanic Hazard (BET_VH, Marzocchi et al., 2010) scheme, to produce long-term probability maps of PDC invasion on the target area, which is among the ones exposed at highest volcanic risk in the world, being densely inhabited and hosting strategical economic infrastructures at national scale. We provide a complete PVHA, that is, we describe both aleatory variability (through a probabilistic description of the variables of interest) and the epistemic uncertainty (through various percentile maps), which is aimed to bound where the true unknown aleatory variability is expected to be (Marzocchi & Jordan, 2014).

Besides a complete characterization of the aleatory variability and epistemic uncertainty, three main novelties characterize this study.

First, in analogy with probabilistic seismic hazard studies (Senior Seismic Hazard Analysis Committee, 1997), the focus of our study is not a single source of hazard, but the target area. In this respect, we account for all the potential sources of the considered hazardous event (PDCs) threatening the metropolitan area of Napoli, that is, Somma-Vesuvius and Campi Flegrei. The total hazard due to both these sources, considering their eruptive activity as mutually independent, is thus evaluated and properly combined. This multivolcano approach represents a major step toward the inclusion of probabilistic hazard studies on PDCs into quantitative risk and multirisk studies, in order to rank risks and prioritize mitigation actions (e.g., Selva, 2013). We remark that in the past, very few studies in volcanology (e.g., Alberico et al., 2011; Lirer et al., 2010) evaluated multivolcano PDC hazard, as the generally accepted approach is to focus on a single volcano. Nevertheless, the studies by Alberico et al. (2011) and Lirer et al. (2010) focused on peculiar events (i.e., single and subjectively adopted scenarios) from each volcano, rather than exploring the natural variability displayed by volcanic activity. In this view, here we fully explore the model parameters' space (for both volcanoes separately) in order to account for all the uncertainties involved. In other words, we do not subjectively choose *representative* scenarios, but we account for all the possible eruption sizes and eruptive vents for both volcanic sources, by adopting a novel approach as regards the eruption sizes recently proposed by Sandri et al. (2016).

Second, we explore wide ranges of flow mobility to consider both dense and dilute PDCs in our hazard analysis, which is entirely based on forward modeling. This includes the quantification of epistemic uncertainty, which, up to now, has been mainly derived from expert judgment (e.g., Neri et al., 2015). In the case of previous BET_VH studies (e.g., Sandri et al., 2012, 2014), epistemic uncertainty was measured in terms of the equivalent sample size Λ (e.g., Selva et al., 2010), the measure being guided by experts' choice. In this study, we compute spatially varying Λ values, using the information contained in the simulations carried out by Tierz, Sandri, Costa, Sulpizio, et al. (2016) and focusing on the largest source of epistemic uncertainty identified by the authors: that is, the theoretical uncertainty.

Finally, since the probability density function (PDF) of the model parameters of the energy cone model is not known, we propose a final hazard assessment based on the ensemble of different hazard assessments (Selva et al., 2014; Tonini, Sandri, & Thompson, 2015); each of them is based on different assumptions on the PDF for the collapse height parameter (H_0). The ensemble aims at evaluating this source of parametric uncertainty (e.g., Rougier & Beven, 2013; Tierz, Sandri, Costa, Sulpizio, et al., 2016).

2. Methods

In order to assess the probabilistic hazard from PDCs invasion, we follow the general scheme of BET_VH probabilistic model (Marzocchi et al., 2010). In particular, we divide the whole process, from the occurrence of an eruption to the impact on a given grid point in the target area, into three main logical steps (e.g., Selva et al., 2014):

1. *Eruption forecasting*—in this step we assess a PDF for the occurrence of an eruption (corresponding to Nodes 1-2-3 in BET_VH) in a given time window, which here we set to 50 years for long-term hazard purposes. For both volcanoes, we use the assessment made in previous studies, that is,
    a. For Somma-Vesuvius, we rely on Marzocchi et al. (2004), who model the long-term probability of eruption in 50 years with a distribution characterized by a mean of about 25% and by a large 90% confidence interval attached ([0.3–80%]).
    b. For Campi Flegrei, we rerun the model proposed by Bevilacqua et al. (2016) based on the last 40-kyr record, to retrieve the full PDF for the probability of at least one eruption in the next 50 years, having a mean value of 38% and a 90% confidence interval of [30–46%]. Worth of notice, the uncertainty attached to this probability is much narrower than in the case of Somma-Vesuvius, probably reflecting the expected "offspring" effect due to the last eruption of Monte Nuovo at Campi Flegrei, as reported by Bevilacqua et al. (2016).
2. *Scenario forecasting*—in this step we build a PDF for the location of the vent, given the occurrence of an eruption, and a PDF for the size of the eruption, given a vent position. These two PDFs respectively correspond to Nodes 4 and 5 in BET_VH.
3. *Impact forecasting*—in this step we assess a PDF for the probability of generating PDCs and reaching a given point in the target area, given the occurrence of an eruption of a given size class and vent. These two PDFs respectively correspond to Nodes 6 and 7 in BET_VH. Since we use a very simple simulator, we are not able to properly compute hazard curves (that would correspond to Node 8 in BET_VH, as in Tonini, Sandri, Costa, et al., 2015).

2.1. Scenario Forecasting

2.1.1. Spatial Probability of Vent Opening

The challenge of mapping the probability of vent opening has been increasingly undertaken by different research groups in recent years, at different volcanic settings such as arcs (e.g., Martin et al., 2004), volcanic fields (e.g., Bebbington & Cronin, 2010), or calderas (e.g., Bevilacqua et al., 2015, 2017; Selva et al., 2010). Here we focus on our two target volcanoes.

2.1.1.1. Campi Flegrei

We use the long-term spatial probability of vent opening proposed by Selva et al. (2012), which was the first one produced and covers the whole Neapolitan Yellow Tuff caldera.

Nonetheless, we also test significant differences in our final results when using a more recent map proposed by Bevilacqua et al. (2015) (see Appendix C). The latter map is quite similar to the former in pattern and values of mean probability (differences bounded to 1–2%); the main differences are that it covers also a part of the larger Campanian Ignimbrite caldera, and it postulates a substantially more concentrated probability of vent opening in the central-eastern part of the caldera, with respect to the estimates of the former map.

We chose the map by Selva et al. (2012) since its full probability density function is available, whereas the one by Bevilacqua et al. (2015) is given in terms of the mean map and two percentiles (5th and 95th) only.

2.1.1.2. Somma-Vesuvius

Previous studies (e.g., Marzocchi et al., 2008a) concentrated most of the vent opening probability at Somma-Vesuvius on the present Gran Cono crater, due to the persistent activity from this vent in the last 2 ka. Here we take a step forward, and by following an approach similar to Selva et al. (2012), we try to use both prior knowledge due to evident features of the volcanic edifice (i.e., summit caldera and Gran Cono) and the location of eruptions in the last ≈22 ka (Cioni et al., 2008).

To do so, we cover the volcano edifice (that we approximate as a circular area with center at (40.821°N,14.426°E) and radius of 6 km, see Figure 1a), with a regular grid of 500-m spacing, totaling N_v=441 grid points. As in Selva et al. (2012), we describe the spatial probability of vent opening by a Dirichlet distribution characterized by a set of parameters $(\alpha_1, \ldots \alpha_{N_v})$ and describing an exhaustive set of N_v mutually exclusive random variates (Gelman et al., 2013); in other words, our distribution for the spatial probability

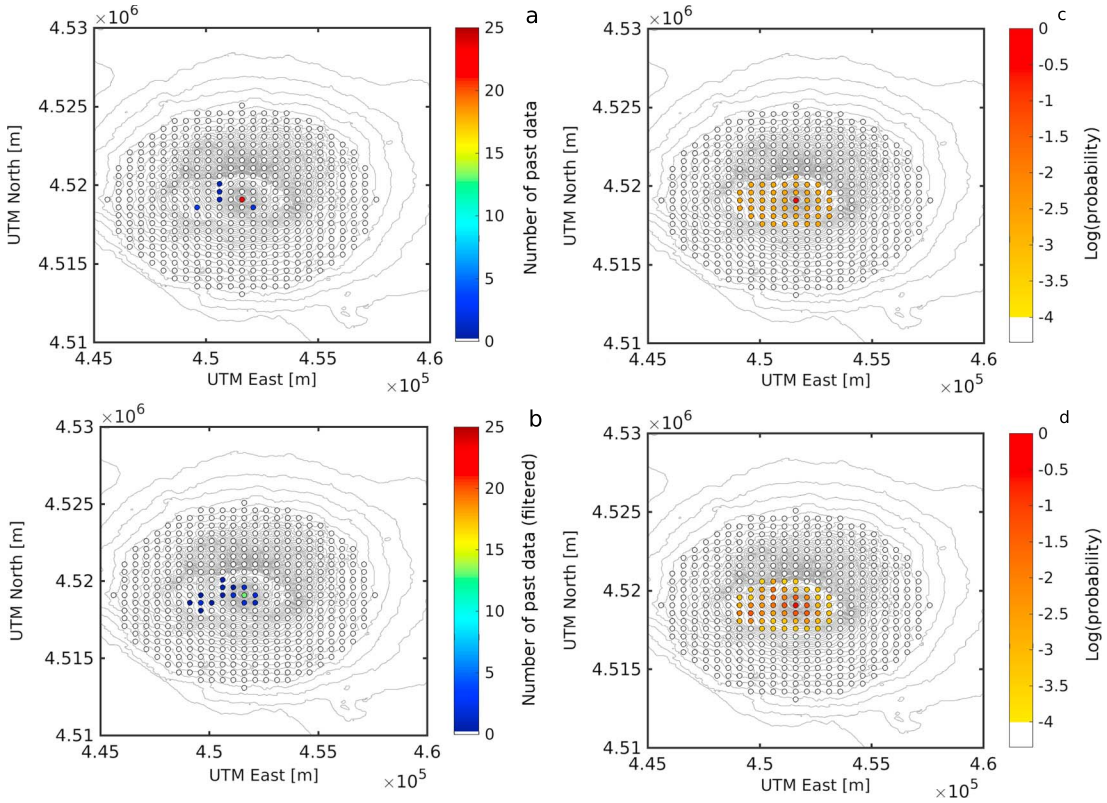

Figure 1. Spatial probability of vent opening, given an eruption, proposed for Somma-Vesuvius (Italy) on the grid of points shown. (a) Number and location of past eruptive vents at Somma-Vesuvius (see Table S1 in the supporting information); (b) number and location of past eruptive vents after applying a Gaussian filter to account for uncertainty in the inferred location for these vents; (c) prior Dirichlet distribution showing high probabilities of vent opening over the present cone and the area covered by past volcanic edifice collapses (summit caldera); (d) posterior Dirichlet distribution computed after updating the prior distribution using the (filtered) past vent locations. Probabilities in (c) and (d) are expressed in Log_{10} scale (values below 10^{-4} are shown in white color).

of vent opening is computed under the assumption that in case of an eruption at Somma-Vesuvius, only one vent will open, and it will be within the area covered by the grid. The set of parameters $(\alpha_1, \ldots \alpha_{N_v})$ fully describe the aleatory and epistemic uncertainty and are univocally linked to the mean probability of each grid points and to a number of equivalent data (or equivalent sample size) Λ, characterizing the dispersion around such mean values (see also Marzocchi et al., 2008b).

In order to assign a prior probability distribution over the grid points, we divide them into three categories: 1 grid point in the center (the Gran Cono's crater), 48 grid points belonging to the area enclosed by previous collapses of the volcanic edifice (we refer to this relatively flat area as "summit caldera", Cioni et al., 1999; Cioni et al., 2008), and the remaining 392 grid points mainly covering the rest of Somma-Vesuvius edifice. We assign a subjective prior mean probability of 0.90 to the crater point and 0.09 to the summit caldera points (uniformly spread, i.e., a mean probability of ~0.002 for each of them); however, in section 3.1, we also test the impact of other plausible prior choices on the posterior map. These prior choices are justified by the inferred location of Somma-Vesuvius's conduit below the Gran Cono position and imply a larger probability of vents over the summit area. They are in agreement with previous works: the one by Marzocchi et al. (2008a), who assigned a general 0.99 probability to the opening of a vent in the summit area of Somma-Vesuvius, and the one by Tadini et al. (2017). However, with respect to the latter, we do not exclude the (unlikely) event of a lateral opening outside the summit area (Gran Cono crater and summit caldera): the lateral points are characterized by a prior mean probability, spread uniformly around all the points, of the remaining 1% (i.e., a mean probability of 2.6 10^{-5} per lateral grid point). A moderate degree of confidence, expressed in terms of equivalent sample size Λ, is given to these prior mean probabilities ($\Lambda = 10$). We then use the location of past Volcanic Exposivity Index (VEI) ≥ 3 explosive events in the last 22 ka (see Table A1 in Appendix A; Cioni et al., 2008) shown in Figure 1a, to condition such prior probability distribution. By using past locations as counts of

Table 1
Parameterization of the Posterior Distributions in the BET_VH Model for Somma-Vesuvius and Campi Flegrei, for Nodes 1 to 6

		Somma-Vesuvius				Campi Flegrei		
Node	PDF	Parameters	Values	References	PDF	Parameters	Values	References
1-2-3	Be	μ_1	0.0026	Marzocchi et al. (2008a)	CH[a]	$1/\lambda_0$	[82; 105; 140]yr	Bevilacqua et al. (2016)
		Λ_1	385			T	[48; 189; 435]yr	
		μ_2	0.5			$\mu_{\text{offspring}}$	[0.26; 0.41; 0.59]	
		Λ_2	1					
		μ_3	0.5					
		Λ_3	1					
4	Di	$\mu_{4\text{min}}$	$7 \cdot 10^{-4}$	This study (see supporting information)	Di	$\mu_{4\text{min}}$	0	Selva et al. (2012)
		$\mu_{4\text{max}}$	0.77			$\mu_{4\text{max}}$	0.048	
		Λ_4	39			Λ_4	29	
5	Di[b]	μ_5	[0.65; 0.24; 0.11]	Sandri et al. (2016)	Di[c]	μ_5	[0.10; 0.61; 0.22; 0.07]	Sandri et al. (2016)
		Λ_5	8			Λ_5	27	
6	Be[d]	μ_6	[0.12; 0.85; 0.80]	Newhall and Hoblitt (2002)	Be[d]	μ_6	[0.92; 0.93; 0.85]	Newhall and Hoblitt (2002)
		Λ_6	[5; 3; 2]			Λ_6	[16; 7; 3]	Orsi et al. (2004)
								Orsi et al. (2009)
								Smith et al. (2011)

Note. For Beta (Be) and Dirichlet (Di) distributions, we provide mean values ($\mu_{\text{node-number}}$) and equivalent sample size ($\Lambda_{\text{node-number}}$). For the PDF describing the probability of an eruption at Campi Flegrei in the next 50 years from Bevilacqua et al. (2016) (Cox-Hawkes process, CH), we use the parameters' names as in that paper.
[a]Values in square brackets correspond to the parameters of triangular distributions as in Bevilacqua et al. (2016). [b]Values in square brackets indicate the parameters for small, medium and large eruption sizes, respectively, at Somma-Vesuvius. [c]Values in square brackets indicate the parameters for effusive, and small, medium and large explosive eruptions, respectively, at Campi Flegrei. [d]Here we used 3 different Beta PDF, one for each eruptive size considered, each describing the probability of generating PDCs, given the eruptive size; in brackets we give the parameters of each Beta PDF, respectively for small, medium and large eruption sizes.

"successes" in a Bernoulli multinomial scheme ($n_1, \dots n_{N_v}$, where n_i is the number of recorded past eruptions in vent position i), we can exploit the conjugacy property of the Dirichlet distribution with the Multinomial function to compute the posterior probability distribution, conditional upon the occurrence of an eruption at Somma-Vesuvius. The posterior distribution is still a Dirichlet, with parameters ($\alpha_1+n_1, \dots \alpha_{N_v}+n_{N_v}$). In practice, since the exact position of some past vents is not known, first we apply a Gaussian filter with null mean and $\sigma = 250$ m (Selva et al., 2012) to the counts of past vents in every possible location. The standard deviation value reflects the expected error in the position of past vents, and it is of the order of the main crater's radius.

Given a number of recorded past eruptions n_j in vent position j, the Gaussian-filtered count n'_j will be

$$n'_j = \frac{\sum_{i=1}^{N_v} w_{ij} n_i}{\sum_{i=1}^{N_v} w_{ij}} \tag{1}$$

where

$$w_{ij} = \exp(-d_{ij}^2/(2\sigma^2)) \tag{2}$$

and d_{ij}^2 is the metric distance between grid points i and j (in case $i = j$, such distance is obviously 0 and the weight $w_{ii} = 1$). The map of the filtered counts is shown in Figure 1b. The resulting posterior distribution is then computed as a Dirichlet distribution with parameters ($\alpha_1 + n'_1, \dots \alpha_{N_v} + n'_{N_v}$).

The list of final parameters of the posterior Dirichlet distribution, and of the corresponding mean probability values, is available in the supporting information.

We also test significant differences in our final results when using a very recent map of the vent opening probability at Somma-Vesuvius proposed by Tadini et al. (2017) (see Appendix C).

2.1.2. Probability Distribution for the Eruption Size

We use the probability distribution for the eruption size proposed by Sandri et al. (2016). In particular, to avoid assuming a set of subjectively chosen representative scenarios, some broad size classes were defined on the basis of different ranges in the total erupted mass observed in the eruptive record of each volcano:

1. For Somma-Vesuvius, three eruption size classes (small, medium, and large, all characterized by explosive activity) were defined by Sandri et al. (2016), assuming that next eruption will require a minimum eruptive energy to reopen the conduit (cf. also Marzocchi et al., 2004).
2. For Campi Flegrei, four size classes (effusive, small explosive, medium explosive, and large explosive) were defined by Orsi et al. (2009).

The small, medium, and large size classes correspond to magnitude ranges respectively 3–4, 4–5, and 5–6 (Pyle, 2000). Then Sandri et al. (2016) built a volcano-specific power law on the total erupted mass in explosive events, constrained by previous occurrences of each size class (see also Table 1). Such power law is here normalized to 1, and then it is sampled to obtain the distribution of total erupted mass in the eruptions originating the PDCs that we simulate. In other words, every simulation performed with energy cone is associated with a specific weight corresponding to its probability according to the total erupted mass attributed to that simulation (which also has an implication on the total height of the eruption column, and thus on the collapse height H_0, as we shall see in section 2.2.2), given the occurrence of an eruption at the considered volcano.

The probability distribution adopted for the eruptive size is independent on the vent position.

2.2. Impact Forecasting

2.2.1. Probability of PDC Generation

Here we use the statistics provided by Newhall and Hoblitt (2002) to define the means of our prior distributions, grouped by eruption size. In agreement with the values reported in the Table 1 in Newhall and Hoblitt (2002), we give the following a priori mean probability values for PDC generation, given an eruptive size or type

1. 0 for effusive eruptions at Campi Flegrei;
2. 0.35 for small size eruptions, at both volcanoes;
3. 0.70 for medium or large size eruptions, at both volcanoes.

We give very low confidence on such prior mean values, assigning a $\Lambda = 1$ (Table 1), thus building up little-informative prior Dirichlet distributions. We then use past frequencies to condition the prior Dirichlet, again in a Bernoulli trial scheme as for the spatial probability of vent opening. In particular, all of the explosive eruptions at Campi Flegrei have generated PDCs; at Somma-Vesuvius all the medium and large size eruptions have generated PDCs, and none of the small size has.

At Campi Flegrei, we also take into account the possibility of a vent opening in the submerged part of the caldera: in such a case, production of subaerial pyroclastic material may be suppressed by the pressure exerted by the water column above the vent (e.g., Lindsay et al., 2010; Sandri et al., 2012; Tonini, Sandri, & Thompson, 2015). Hence, whatever the explosive size class, we first assume that PDCs are not generated if the vent opens at a depth larger than 10 m. We then test the sensitivity of our results to such choice by adopting the empirical approach by Tonini, Sandri, & Thompson (2015), that is, by assuming a linear decay in the probability of generating explosive activity, and thus PDCs, as the water depth increases.

2.2.2. Probability of PDCs Reaching Target Grid Points

2.2.2.1. Approach to Simulations

As regards the probability of PDCs reaching a given target point, we make use of simulations performed specifically with the energy cone model that are illustrated in this section. The general approach is the same one adopted by Tierz, Sandri, Costa, Sulpizio, et al. (2016) and Tierz, Sandri, Costa, Zaccarelli, et al. (2016); for every volcano, vent position, and size class, we first define a suitable model parameter space and distribution for the energy cone parameters, collapse height (H_0), and PDC mobility (ϕ; the smaller the ϕ value, the larger the mobility). We highlight that such parameter space is built up blindly with respect to our final measure of hazard, that is, the PDCs invasion area: it is built up on the basis of independent data, coming from analog volcanoes (see below).

We then sample tens of thousands of pairs of values from this parameter space, and for each pair, we run an energy cone simulation. Finally, at each grid point, we compute the frequency of simulations that reach the point, and this is adopted as our best estimate value (the mean) of the probability of PDC invasion at that grid point.

2.2.2.2. Mobility: The ϕ Angle

In this study, we sample the mobility ϕ from truncated Gaussian and uniform distributions for Somma-Vesuvius and Campi Flegrei, respectively, as in Tierz, Sandri, Costa, Zaccarelli, et al. (2016, specifically in their Figures 3b and 3d; see more details in the paper). These two distributions reflect the different amount of data available for PDCs generated by volcanoes that are analog to our test volcanoes: there are many more observations from volcanoes which are analog to Somma-Vesuvius than to Campi Flegrei. For Somma-Vesuvius, we mostly rely on the worldwide data set of ϕ values by Ogburn (2012), which is fitted by a truncated Gauussian PDF. For Campi Flegrei, we lack such a database, and therefore, we select a very noninformative distribution (uniform PDF).

2.2.2.3. Collapse Height H_0

To achieve adequate samples for the collapse height, we follow an analogous procedure to the one adopted in Tierz, Sandri, Costa, Zaccarelli, et al. (2016). In particular, we first sample the total height of the eruption column from the distributions proposed by Sandri et al. (2016), for each size class and for the two volcanoes separately. In that work, given an eruptive size class and volcano, the total height of the eruption column was a random variable deriving from a stratified sampling procedure in which a total erupted mass and eruption duration (hence the mean mass eruption rate) were sampled from respectively a power law and a uniform distribution, both consistent with field data for that volcano. The total height of the eruption column was then computed according to Mastin et al. (2009) through the mean mass eruption rate of the fallout phase, considering a reasonable mass fraction associated to that phase (80% and 25%, respectively, for Somma-Vesuvius and Campi Flegrei from the available estimations from field data analysis; see Sandri et al., 2016, and references therein). Once the sample of total heights of eruption column is available from Sandri et al. (2016), as in Tierz, Sandri, Costa, Zaccarelli, et al. (2016), we assume that collapse will occur within the gas thrust region whose top can be roughly estimated as 10% of the total height of eruption column (Wilson et al., 1978). The last step is to sample a random collapse height H_0 from each gas thrust region. As a novelty with respect to Tierz, Sandri, Costa, Zaccarelli, et al. (2016), here we explore how results change when considering two "end-member" assumptions on the type of probability distribution used to sample the collapse height H_0 from the height of the gas thrust region. In particular, we run two separate sets of simulations considering:

1. A truncated exponential probability distribution on the height of the gas thrust region (as in Tierz, Sandri, Costa, Sulpizio, et al., 2016; Tierz, Sandri, Costa, Zaccarelli, et al., 2016) reflecting the idea that large column collapse heights are less likely than smaller ones (a common feature of frequency-size relationships in nature, e.g., the Gutenberg-Richter law for earthquakes)
2. A uniform probability distribution on the height of the gas thrust region, reflecting maximum ignorance on the real relative frequency of large to small collapse heights.

The results of the two simulation sets are then merged together to compute an ensemble hazard model, which is a statistical mixing in which we give equal weight to the two end-member assumptions. In Appendix B we provide a detailed description of the evidence upon which we build up the two different probability distributions.

2.2.2.4. Confidence on Best Estimate of PDC Invasion Frequency: A Spatially Varying Equivalent Sample Size Λ

Further, we use subgroups of simulations to infer the confidence (the Λ value for this node) on the best estimates of frequency of PDC invasion at each grid point. As mentioned in section 1, Tierz, Sandri, Costa, Sulpizio, et al. (2016) found that the largest contribution to epistemic uncertainty on invaded area and maximum runout, when using the energy cone model, comes from alternative hypothesis on possible correlations between values of H_0 and ϕ, namely, a "direct" correlation (the largest the H_0, the more mobile the flow, and thus the smaller the ϕ angle, and vice versa, e.g., Doyle et al., 2010), and an "inverse" one (the largest the H_0, the less mobile the flow and thus the larger the ϕ angle, and vice versa, e.g., Esposti Ongaro et al., 2008). In order to assess how well constrained our best estimate frequency of PDC invasion is, we extract two subgroups from our simulations; each subgroup has model parameters' pairs in agreement with either one of the two correlation patterns: the subset of pairs in agreement with the direct pattern (in which the H_0 values are either below the 20th percentile or above the 80th percentile, and the corresponding ϕ values are respectively either above the 80th percentile or below the 20th percentile) and the subset of pairs in agreement with the inverse pattern (in which the H_0 values are either below the 20th percentile or above the 80th percentile, and the corresponding ϕ values are respectively either below the 20th percentile or above the 80th percentile). Both the direct and inverse pattern "share" model

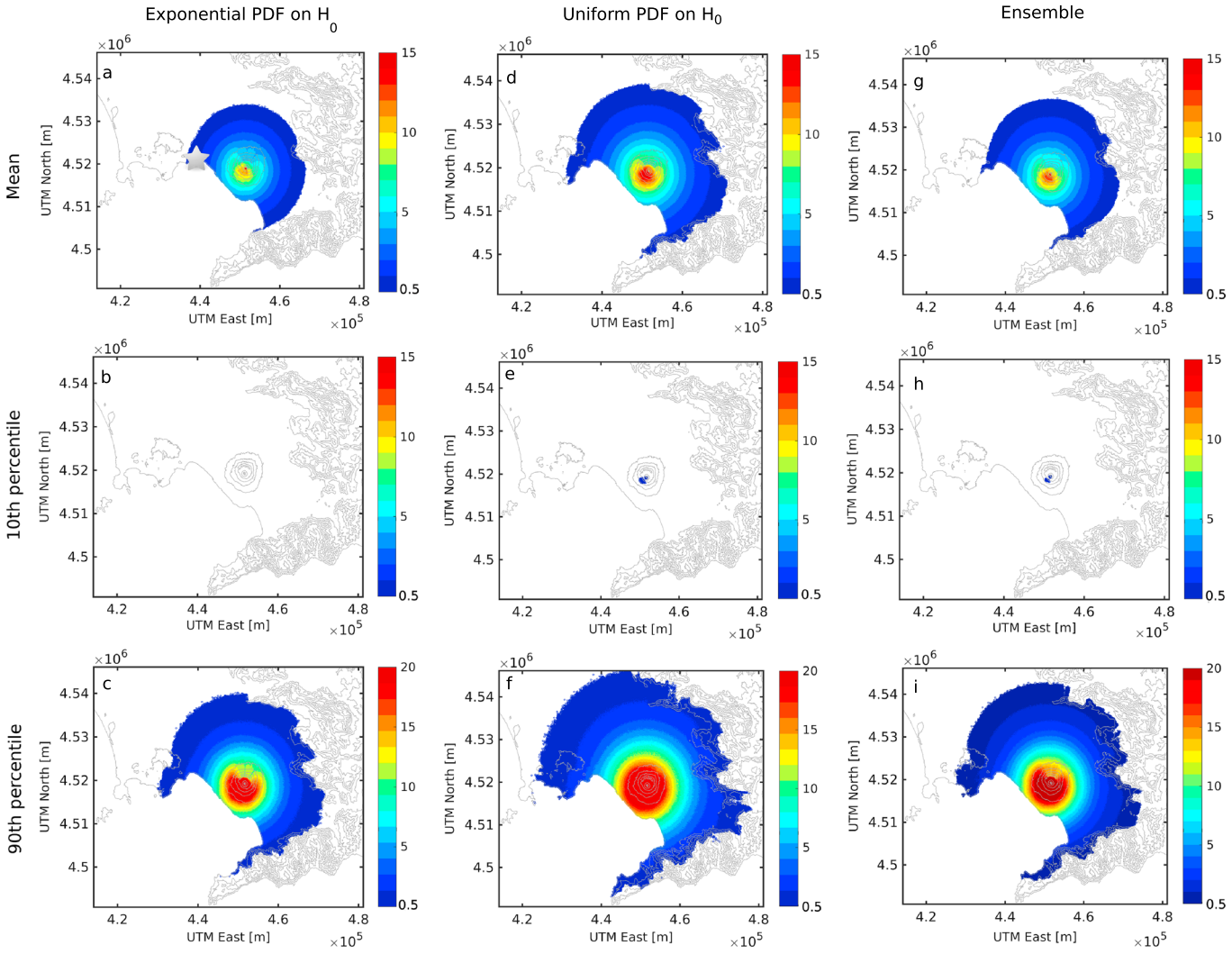

Figure 2. Probability maps displaying the probability (or future frequency) of pyroclastic density currents, from Somma-Vesuvius, arriving at each grid point over the hazard domain (the light gray star points downtown Napoli) in the next 50 years, according to the exponential probability density function (PDF) for collapse height (a, b, and c respectively show the mean, 10th, and 90th percentiles), the uniform PDF for collapse height (d, e, and f respectively show the mean, 10th, and 90th percentiles), and their ensemble model (g, h, and i respectively show the mean, 10th, and 90th percentiles). Note that only probability values above 0.5% in 50 years are displayed, and that the color scale on panels c, f, and i is different, and it saturates (e.g., maximum values are around 40% for the ensemble).

parameters' pairs that are located between the 20th and 80th percentile of both H_0 and ϕ. In this way, the subsets are continuous in terms of the model parameter values (Tierz, Sandri, Costa, Sulpizio, et al., 2016). Therefore, we are able to compute two additional values for the frequency of PDC invasion, at each grid point, according to the simulations belonging to the two subgroups. In the end, for a given target grid point, we obtain three values for the frequency of PDC arrival: one considering all the simulations and two considering the theoretical uncertainty on the link between the energy cone parameters. We best fit these three values with a Beta distribution, thus retrieving the best estimate value for the frequency, and an associated Λ value (equivalent sample size). At a given target grid point, these two values fully define the Beta distribution for the Node 7 in BET_VH (for every volcano, vent position, and size class).

2.3. Ensemble Probability of Invasion From Each Volcano, and PVHA in 50 Years

For both volcanoes (Somma-Vesuvius and Campi Flegrei), after having set the probability distributions at all the nodes of BET_VH, and for any given grid point in our hazard domain, we sample 1,000 variates from these distributions at each node and combine them to obtain 1,000 values of the probability of PDCs invading that grid point. We repeat this for both the end-member assumptions on the PDF governing the collapse height parameter of the energy cone model (exponential and uniform) and obtain two different maps of the

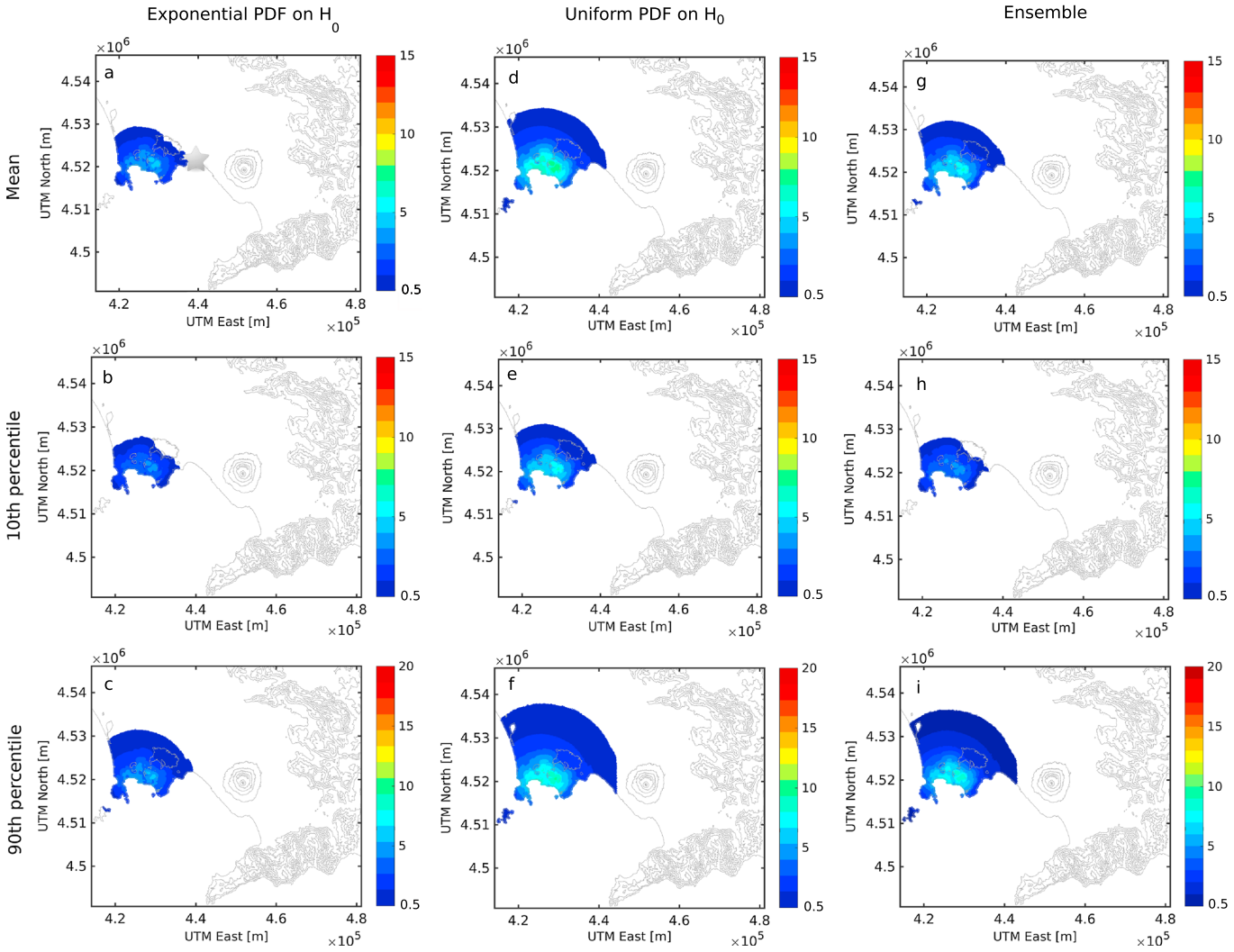

Figure 3. Same as Figure 2, but for pyroclastic density currents from Campi Flegrei. Maximum value for 90th percentile (panels c, f, and i) here is around 10% and does not saturate the color bar scale. PDF = probability density function.

probability of invasion by PDCs in 50 years, for each volcano. The two maps quantify the parametric uncertainty arising from the unknown shape of the PDF for H_0. In order to obtain a single probability map for every volcanic source, these two maps are statistically mixed, with equal weight, to obtain the ensemble probability of invasion in 50 years (Figures 2 and 3, respectively, for Somma-Vesuvius and Campi Flegrei).

Finally, we combine the two volcanic sources by assuming that they erupt independently. That is, at any given grid point *i*, we compute the probability of experiencing PDCs from *at least* one of the two volcanoes in the next 50 years ($PVHA_i$) through the equation

$$PVHA_i = 1 - (1 - PVHA_{SV_i}) \cdot (1 - PVHA_{CF_i}) \quad (3)$$

where $PVHA_{SV_i}$ and $PVHA_{CF_i}$ are the probabilities of PDC invasion, at grid point *i* and in the next 50 years, from Somma-Vesuvius and Campi Flegrei, respectively. The resulting PVHA maps are given in Figure 4.

3. Results

3.1. Vent Opening Probability at Somma-Vesuvius

In Figures 1c and 1d we show respectively the prior and the posterior distribution (mean values) for the spatial vent opening probability at Somma-Vesuvius. Compared to the one by Tadini et al. (2017), our map covers the whole volcanic edifice (although with very low probability values) and not only the summit caldera; further, our description of the summit caldera shows that the Gran Cono crater is much more likely to be the location of future vents (as 21 out of the 29 eruptions considered in Table A1 in Appendix A are inferred to have occurred

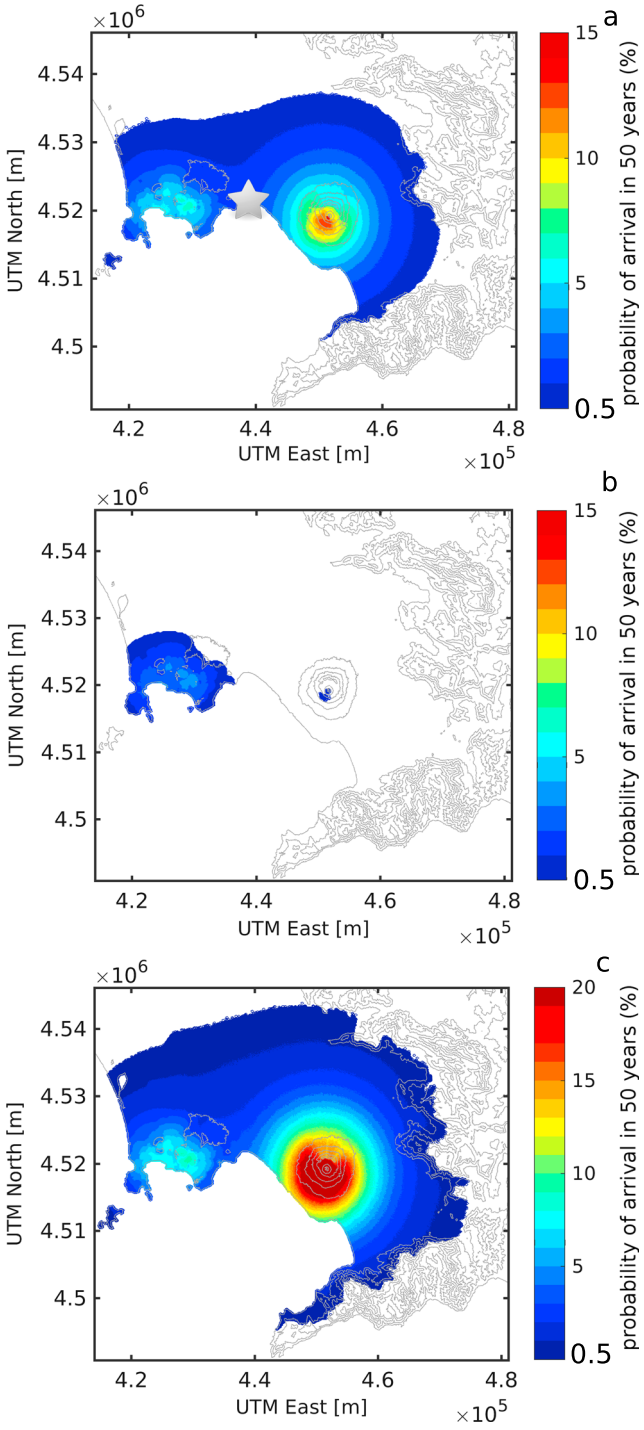

Figure 4. Multivolcano probability maps displaying the probability (or future frequency) of pyroclastic density currents arriving at each grid point over the hazard domain (the light gray star points downtown Napoli) in the next 50 years, according to the ensemble models for H_0 for both volcanic sources (a, b, and c respectively show the mean, 10th, and 90th percentiles). Maximum values for 90th percentile (panel c) are around 40% and 9% in the proximal areas of Somma-Vesuvius and the eastern part of the Campi Flegrei caldera, respectively.

from the Gran Cono). In contrast, the map by Tadini et al. (2017) is almost a uniform map on the area of the summit caldera. However, we remark that the map by Tadini et al. (2017) was built on, and for, VEI ≥ 4 eruptions, while here we consider also smaller events.

In order to test the importance of our prior subjective choices (mean probability of 0.99 on the summit area and 0.01 globally on the lateral points) on the posterior map, we also try two different prior mean values' configurations: one with 0.95 given to the summit area (0.85 to the crater point, 0.10 to the summit caldera points) and 0.05 globally to the lateral points; another one with 0.90 given to the summit area (0.80 to the crater point, 0.10 to the summit caldera points) and 0.10 globally to the lateral points. In both cases, the resulting differences in the posterior map are practically confined to the lateral points, being of the order of 10^{-5} (less than an order of magnitude in relative terms). This is due to the dominant information carried by the likelihood function, built on the vents formed during the last 22 ka of the volcano's history.

3.2. Probability of PDC Arrival

In Figures 2 and 3 we show the probability of invasion of PDCs in all the grid points in the next 50 years, at different percentiles (the best estimate value given by the mean, and epistemic uncertainty expressed by 10th and 90th percentiles, that is, an 80% confidence interval), for Somma-Vesuvius and Campi Flegrei, respectively and separately. These results are shown for both the end-member assumptions on the distribution governing H_0 (exponential and uniform), and in terms of their statistical mixture (i.e., the ensemble with equal weight, see previous section 2.3).

Obviously, at any given point the ensemble value lies in between the two end-members, being the model based on a collapse height drawn from a uniform PDF always providing a higher probability of invasion than the one based on exponential.

3.2.1. Single Volcano: Somma-Vesuvius

At Somma-Vesuvius, the highest probabilities of PDC arrival are observed over the southern flank of the volcano, with mean values around 10% in 50 years for the ensemble, extending for about 4 km toward the southwest (Figure 2). For the model based on the uniform PDF, the highest mean probability around the summit area is about 15% in 50 years. The shape of Mount Somma is mapped, very neatly, by the northern limit of the isoline of mean probability corresponding to 8% (Figure 2d). Moreover, the central, most elevated part of Mount Somma is evidenced by the shape of the 6–8% color contouring toward the north. No point in the map has a 10th percentile of the PDF describing the frequency of PDC arrival in 50 years above 0.5% (Figure 2a). In contrast, according to the 90th of such PDF, areas up to 10^3 km^2 are covered by probabilities of PDC arrival, in the next 50 years, greater than 0.5%. Nevertheless, the probabilities over medial or distal sectors (beyond ~8 km) are below 5% and confined by the Appenninic topographic over the S-SE and N-NE (Figure 2b).

The values of probability of PDC arrival toward the west must be taken with extreme care: the energy cone model is not suitable to model PDC propagation over the sea water (e.g., Cordoba, 2007, see also discussion in section 4.4).

The analysis of differences in the percentile maps indicates that the summit part of Somma-Vesuvius has an 80% confidence interval approximately [0.5%–40%] in 50 years; the same quantities, for PDCs generated from Somma-Vesuvius invading the city center of Napoli (gray star in Figure 2) are between [0.02%–2%], with a mean value of 1% (Figure 2).

3.2.2. Single Volcano: Campi Flegrei

At Campi Flegrei, the maximum probability of PDC invasion according to the ensemble model, in the next 50 years, is about 7% (mean value) and ranges between [4%–9%] (80% confidence interval) when epistemic uncertainty is taken into consideration. For the model based on the uniform PDF, the highest probability is about 9% in 50 years. These maxima in probability of PDC arrival are located in the Eastern caldera sector, in particular over the Astroni crater and the Agnano plain (Figure 3d). The general spatial pattern of the mean probability of PDC arrival shows that values equal to or greater than 3% (in 50 years) are restricted to the structural boundaries of the calderas formed during the Campanian Ignimbrite and the Neapolitan Yellow Tuff (e.g., Deino et al., 2004; Fedele et al., 2003, and references therein). Nonetheless, in our maps the gradient in the mean probability values is not extremely sharp across the caldera's boundary: for example, the Posillipo hill (located beyond the Eastern border of the Neapolitan Yellow Tuff caldera, and part of the municipality of Napoli) has a mean probability of 2–3% to be hit by PDCs from Campi Flegrei. At the city center of Napoli (gray star in Figure 3), mean probabilities of PDC arrival are around 1% and [0.01%–2%] considering the aforementioned 80% confidence interval. At farther distances, mean values of probability of

PDC arrival ≥0.5%, in 50 years (colored contouring), are obtained for grid points up to 10–12 km from the center of the Campi Flegrei caldera (Figure 3c). When accounting for epistemic uncertainty, in this case the dispersion around mean values is much less, due to the quite informative model by Bevilacqua et al. (2016) that we use to describe the temporal occurrence of eruptions at Campi Flegrei at node 1: as mentioned in section 2, the 90% confidence interval associated to the mean value, describing the epistemic uncertainty attached to the probability of eruption in the long term, is much larger for Somma-Vesuvius than for Campi Flegrei. As a consequence, the differences between maps in Figures 3a and 3b are not so marked as for Somma-Vesuvius, and probability of PDC arrival can range from maxima less than 5% and confined to the Neapolitan Yellow Tuff caldera (10th percentile in Figure 3a) to values generally greater than 5% over such caldera and values above 0.5% at distances of about 15 km (northward, for instance) from the center of the caldera (90th percentile in Figure 3b).

We also test how our probability maps for PDCs invasion change when dropping the assumption of total suppression of explosivity if the vent is submerged and deeper than 10 m. To this end, we rerun our scheme by assuming that the probability of PDCs generation, in such a case, linearly decreases as in the empirical model proposed by Tonini, Sandri, & Thompson (2015): for small, medium, and large eruptions, the probability of PDCs generation starts decreasing when the submarine vent is 10-m deep and becomes null when the vent is respectively 100, 200, and 300-m deep, considering the empirical data by Mastin and Witter (2000). We observe that the changes in the final probability maps are negligible, with respect to what shown in Figure 3.

3.2.3. Multivolcano Hazard Model

In Figure 4, we show the map of the combined PDC hazard calculated for the activity at the two volcanoes, assumed to erupt independently, based on the single volcanoes' ensemble models. Thus, the probability of PDC arrival displayed in this figure corresponds to the probability of PDCs, from at least one of the two volcanoes, invading each grid point over the central Campania region. These multisource probability maps are very similar to the single-source maps (Figures 2 and 3) in the vicinity of each volcano, as far as the PDCs from one of them are not able to propagate far enough to invade grid points over the proximal sector of the other volcano, apart from some unlikely cases (Figures 2 and 3). The city of Napoli has its western part located on the Campi Flegrei caldera and its center and eastern part in between the two volcanoes. The probabilities of PDC arrival (in 50 years) shown in Figure 4 are obviously greater than the probabilities computed from either single volcanic source (see equation (3)). In particular, the whole city center is placed over grid points with mean probability of PDC arrival, in 50 years, of about 2%. These mean values reach 3–4% over the eastern end of the city and 4–5% over the western areas of the municipality inside the Campi Flegrei caldera (Figure 4a). According to the 10th percentile of the distribution for the probability of PDC arrival (in 50 years), the city of Napoli downtown is less than 0.5% probable to be impacted by PDCs in the next 50 years (Figure 4b). However, if the 90th percentile of the distribution is considered, it is associated with values around 4% in 50 years, while the western sector of the city is about 8% probable to be impacted by PDCs (Figure 4c).

4. Discussion

4.1. PVHA Results

Even though the PDCs from Campi Flegrei tend to be more mobile than the ones from Somma-Vesuvius (Gurioli et al., 2010; Orsi et al., 2004; Tierz, Sandri, Costa, Zaccarelli, et al., 2016), the summit and southern flank of Somma-Vesuvius are more likely to experience PDC invasion than any other point along the hazard domain. This is mostly due to two reasons. First, there is a "dissipating" effect caused by the much larger uncertainty on the vent position at Campi Flegrei: while the distance between any given grid point within the Campi Flegrei caldera and the next opening vent is very uncertain (it can range from meters to kilometers with similar probability, e.g., Bevilacqua et al., 2015; Selva et al., 2012), the points nearby the Somma-Vesuvius summit are highly likely to be close to the next opening vent, as Somma-Vesuvius summit caldera area concentrates almost all the probability of vent opening (Figure 1d and Tadini et al., 2017). Second, the predominant topographic structure of Somma-Vesuvius stratovolcano allows PDCs to propagate, at least, toward the south and west where there is no barrier. On the opposite, in our simulations, the rough topography of the Campi Flegrei caldera often stops small PDCs (by far the most likely ones, at least in the case of H_0 being sampled from an Exponential distribution) close to their originating vent. In other words, PDCs from Campi Flegrei are entrapped by neighboring topographic heights at short distances from the point they originate, hence reducing the

Table 2
Summary of the Probability of PDC Invasion, in the Next 50 years, for Downtown Napoli As Well As the Eastern and Western Areas of the City, Using the Ensemble Hazard Model for a Single Volcano (Somma-Vesuvius, SV, and Campi Flegrei, CF) or for Both the Volcanoes (i.e., Multivolcano Hazard Model)

	Ensemble SV mean [80% CI]	Ensemble CF mean [80% CI]	Ensemble multivolcano mean [80% CI]
Downtown Napoli	1 [0.02; 2]	0.7 [0.02; 2]	2 [0.3; 4]
Eastern Napoli	3 [0.08; 7]	0.2 [0; 0.5]	3 [0.2; 8]
Bay Western border (Posillipo)	0.4 [0.005; 1]	2–3 [0.1; 7]	2–3 [1; 5]

Note. We report both a measure of aleatory uncertainty (mean probability values) and epistemic uncertainty (e.g., 80% confidence interval, CI, between the 10th and 90th percentiles of the distribution associated with this probability). All probabilities are expressed in percentages.

probability of PDC invasion over medial/distal sectors from each vent. This is in relative disagreement with recent PVHA studies carried out at Campi Flegrei (Neri et al., 2015). We further discuss this aspect in section 4.3 and Appendix D.

Furthermore, it is key to analyze how the probability of PDC invasion increases when the novel multivolcano hazard model is used. This type of approach has been applied to other volcanic hazards (e.g., tephra fallout, Jenkins et al., 2012) and represents a crucial step forward for volcanic hazard assessment in inhabited areas threatened by more than one volcano. In Table 2, we compare the PVHA at three different sites in the municipality of Napoli (downtown, the eastern side, and Posillipo Hill on the western border of the Napoli bay) achieved by considering the two volcanoes separately and together. As expected, the largest effect is at the city center of Napoli, lying at the "intersection" of the two hazard sources: here the mean probability doubles when considering multiple sources. On the contrary, the eastern and western borders of the bay are much less affected by the corresponding farthest volcanic source. The effect of the multivolcano assessment on the epistemic uncertainty is less intuitive: on the whole, we see that the 80% confidence intervals are wider in the multivolcano hazard model, even though the lower bound of the 80% confidence interval (i.e., the 10th percentile) is about 1 order of magnitude higher than those of the single-volcano hazard models (Table 2).

4.2. Objective Quantification of Spatially Varying Equivalent Sample Size

Our novel approach of quantifying, at each grid point, the equivalent sample size (Λ in Marzocchi et al., 2008a, 2010) for Node 7, which is based on the simulations of the physical model (instead of deriving it from expert judgment, e.g., Sandri et al., 2012, 2014; Selva et al., 2010), allows analyzing the spatial patterns in this BET_VH parameter. Therefore, areas where epistemic uncertainty (in our case, theoretical uncertainty, see section 2.2.2) is high (i.e., low Λ values; minimum Λ is 1) or low (i.e., high Λ values; maximum Λ shown is 1,000) can be identified and related to the main morphological features of the two volcanoes. In Figure 5, we show the spatial distribution of $\log_{10}(\Lambda)$ for different eruption sizes from the most probable vent location at Somma-Vesuvius (central summit crater) and Campi Flegrei (Astroni crater).

At Somma-Vesuvius, the maps are characterized by a region of low uncertainty (yellow ring for medium and large size, proximal area to the SE for the small size) which is where the three patterns (independent, direct, and inverse) in the energy cone parameters that define theoretical uncertainty lead to similar output frequencies of PDC arrival (Figures 5a–5c). We interpret this zone as the one having an approximately equal number of simulations with smaller and larger model parameter values (H_0, ϕ). In this view, half of the simulations produce shorter runouts (or smaller areas of PDC invasion) and the other half produce larger runouts (or larger areas of PDC invasion). The in-between zone, characterized by frequencies around 50%, is reached with a similar frequency no matter the relationship between H_0 and ϕ. The location of this zone of minimum epistemic uncertainty is size dependent, as observed in Figure 5. For the medium eruption size (Figure 5b), its northern limit is located at the base of Mount Somma, highlighting the importance of this topographic barrier for medium-size PDCs (e.g., Esposti Ongaro et al., 2008; Neri et al., 2008). In other words, in medium-sized eruptions the proportion of PDCs able to overcome Mount Somma is more uncertain than the proportion of PDCs that may reach the base of this topographic barrier. PCDs generated in large-size eruptions are, in turn, (Figure 5c) less influenced by Mount Somma, and the low-uncertainty yellow zone is located some kilometers away from the barrier. Additionally, the maps for the small and medium eruption sizes (Figures 5a and 5b) also

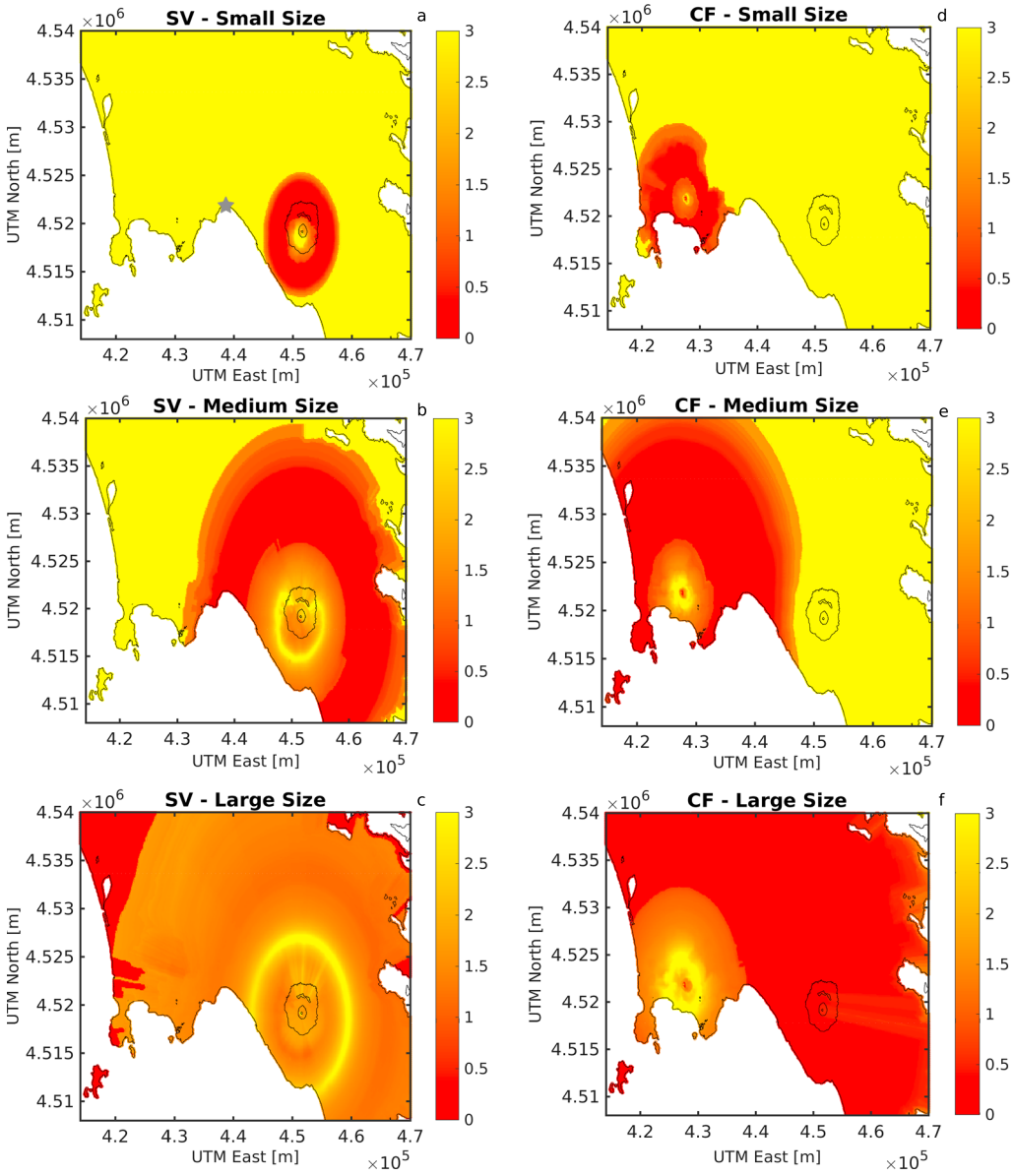

Figure 5. Spatially varying equivalent number of data used to parameterize the Beta probability density functions (there is one probability density function per each grid point) for Node 7 of the BET_VH model. The displayed values are computed by exploring theoretical uncertainty via the energy cone model (after Tierz, Sandri, Costa, Sulpizio, et al., 2016) for three eruption sizes and two volcanoes (Somma-Vesuvius [SV] and Campi Flegrei [CF], in Italy). The maps for Somma-Vesuvius (a–c) are based upon energy cone simulations starting from the current central crater of the volcano while those for Campi Flegrei (d–f) correspond to energy cone simulations starting from the closest vent position to the Astroni crater.

show a further low-uncertainty zone (i.e., high Λ) at large distances from the central crater due to the fact that no simulated PDCs (of these sizes) is able to invade those distal grid points.

At Campi Flegrei (Figures 5d–5f), maps are characterized by a low-uncertainty zone surrounding the Astroni crater: the larger the eruption size, the wider this zone. We interpret this zone as an effect of topography, and in particular as the zone invaded by all the PDCs that make it out of the Astroni crater. Inside the crater itself, the variability is a bit larger (reddish colors) as very small PDCs probably do not invade all of the crater area. Again, at large distances from the crater, there is a low-uncertainty zone that is where no simulated PDCs arrive. According to our results, the simulated PDCs are not strongly confined by the presence of the scarps that delineate the boundaries of the Campi Flegrei caldera (e.g., Orsi et al., 2004; Neri et al., 2015).

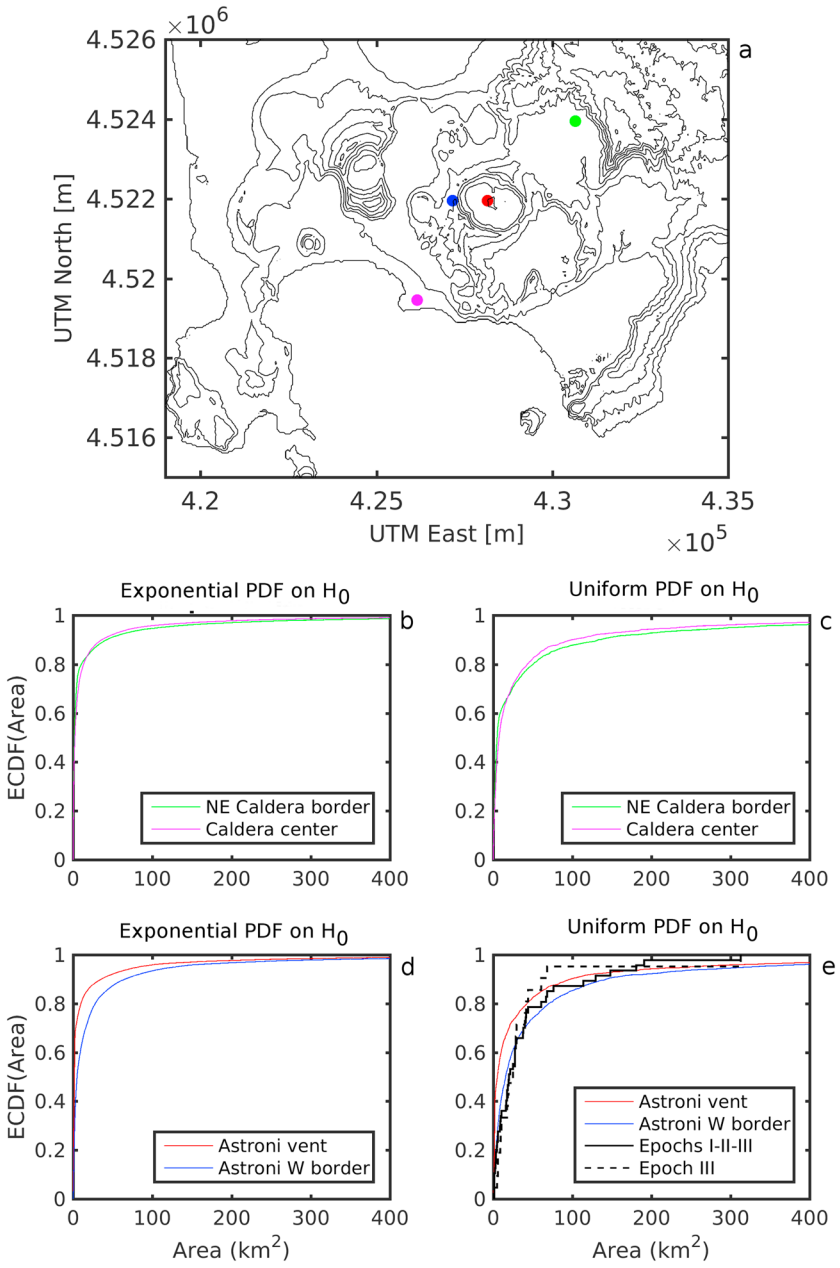

Figure 6. (a) Campi Flegrei topography map, with highlighted a few selected possible vent positions on which we build the empirical cumulative distribution function of the probability density function (PDF) invaded areas according to our energy cone simulations. Green, magenta, red, and blue points are respectively northeast border of caldera, Pozzuoli (caldera center), Astroni vent bottom, and its Western outer border. In (e) we also show the empirical cumulative distribution function from Neri et al. (2015) both for Epoch III only (dashed black line) and for all Epochs together (solid black line).

In other words, a certain (albeit small, Figure 3) number of PDCs are able to overcome the caldera boundaries and invade grid points toward the north. Therefore, the epistemic uncertainty at the caldera boundaries and beyond is relatively high (Figures 5d–5f).

4.3. Comparison With Previous PDC Hazard Assessments at the Target Volcanoes

Our final probability maps in Figures 2–4 represent a unique PDC hazard assessment for the city of Napoli and surroundings, and therefore, they cannot be really compared with previous works, even in the case of a single volcanic source. That is, for each volcano analyzed (Figures 2 and 3) and for the two volcanoes jointly

(Figure 4), our maps display the probability of PDC invasion, in a specific time window, from an eruption of any size and from any possible vent.

Nonetheless, by using BET scheme, we can extract other results from our simulations: maps of PDCs invasion conditional upon the occurrence of an eruption, or to the occurrence of an eruption of a specific size, or from a specific vent. These further maps can be compared to those from previous studies, as detailedly discussed in Appendix D. Here we sum up briefly the main outcomes of such comparisons. At Somma-Vesuvius we observe a statistical consistency between our mean probability map of PDC invasion with the frequency extracted from field deposits of PDCs (Gurioli et al., 2010), and a broad agreement with the main results by Neri et al. (2008). At Campi Flegrei, we compare our results with those by Neri et al. (2015). Our expected frequency of PDC invasion given an explosive eruption from the emerged part of the Campi Flegrei caldera (as in Neri et al., 2015) is generally lower than that computed by Neri et al. (2015) (maximum difference, located in the Eastern part of the caldera, is approximately 40% and 30%, respectively, when using the exponential and uniform PDF to describe the collapse height). We interpret such differences as linked to one (or a combination) of the following causes:

1. The empirical statistical distribution of the areas invaded by PDCs, used by Neri et al. (2015) to construct their probability maps, is conditional upon the actual position of the eruptive vents in the past; however, the authors sampled the same statistics to simulate PDC invaded areas associated with any vent position along the whole (inland) caldera.
   To check whether the statistical distribution of the PDC invaded areas is independent on the actual position of the vent, we compute the empirical cumulative distribution function (ECDF) of the invaded areas according to our simulations when considering eruptive vents located in different portions of the Campi Flegrei caldera (see Figure 6a); in particular we examine vents close to the border or in the center of the caldera (green and magenta dots, respectively) or vents characterized by different surrounding topography (e.g., Astroni vent: bottom of the crater or outer border, red and blue dots, respectively). To do so, given the energy cone simulations from one of these vents, we compute the inland PDC invaded areas in each simulation, and then we compute the ECDF from the given vent by weighting each simulation with the probability of its eruptive size (we remind that the statistical distribution sampled by Neri et al., 2015, includes all the eruptions found in the field deposits, regardless of the eruptive size). Afterward, we statistically compare the ECDF from different vents through a two-sample Kolmogoroff-Smirnov test, rejecting at 5% significance level the null hypothesis (i.e., the sets of PDC invaded areas from different vents being samples originating from a common underlying distribution) in all of the cases shown in Figure 6a: in other words, at Campi Flegrei the simulated PDC invaded area depends on the position of the vent. This is true for simulations from both end-member assumptions on the collapse height. The most dramatic difference, among the inspected cases, is when we compare the invaded areas from the center of Astroni vent (red dot in Figure 6a) to those from a vent just outside its border (blue dot). In the latter case, the invaded areas are much larger than in the former (Figures 6d and 6e). In this view, the statistical comparison of the ECDF of the PDC invaded areas in the third epoch, or all the three epochs (shown in Figure 6e as an example), with that extracted from our simulations, without accounting for the vent position, appears pointless.
2. The largest majority of our simulations provide lower values for the invaded areas with respect to the data listed by Neri et al. (2015) (see Figure 6e as an example: very small invaded areas are much more likely from our simulations than in real data). However, the field data used to construct the empirical ECDFs in Neri et al. (2015) might suffer from underrecording, especially of small-size eruptions (e.g., Rougier et al., 2016)) that can leave minor erodible PDC deposits (e.g., Druitt, 1998); in this respect, we find interesting to observe that PDCs formed during many small eruptions at Campi Flegrei have preserved maximum runouts comparable to the maximum runouts of PDCs formed during medium eruptions (see Figure 7a in Tierz, Sandri, Costa, Zaccarelli, et al., 2016).

Two final significant differences of our work with respect to previous multivolcano hazard assessments (e.g., Alberico et al., 2011; Lirer et al., 2010) are the following. First, we consider all possible eruption sizes and eruptive vents, combined through the total probability theorem, without selecting a reference size or scenario as in Lirer et al. (2010) and Alberico et al. (2011), who, for example, selected a reference eruption size (a VEI = 4 for Campi Flegrei) or specific past eruptions (only the PDC deposits from the Avellino, 79 AD and 472 AD Pollena eruptions for Somma-Vesuvius). Further, and more important, our maps provide numerical values of the probability of PDC arrival in the next 50 years, which can be interpreted as expected frequencies (Marzocchi & Jordan, 2014) and can be used by decision makers as input for rational decisional protocols (e.g.,

cost-benefit analysis, Marzocchi & Woo, 2007, 2009) without any subjective discretization made by scientists. Conversely, in Alberico et al. (2011) and Lirer et al. (2010) the volcanic hazard is dicretized into "low," "medium," and "high" hazard areas, making impossible the application of a sound decision making rooted in quantitative cost-benefit analysis and implicitly violating the hazard-risk separation principle advocated in other fields (e.g., Jordan et al., 2014).

4.4. Limits of our Model

Energy cone model postulates a linear loss in the energy of PDCs with distance from the vent, depending simply on the elevation of the eruption column collapse from which the PDC is originated and on a friction angle describing its bulk mobility. Obviously, several further parameters influence PDCs mobility, such as particle volumetric concentration and particle mass flow rate. Being aware of this intrinsic simplicity of the model, we still make use of the energy cone model in this study for different reasons:

1. In Tierz, Sandri, Costa, Zaccarelli, et al. (2016) it was shown the statistical agreement (see section 1) between the energy cone outputs, when the model is run in a Monte Carlo scheme with input parameters sampled from blindly defined parameters' space, and the observations available at Somma-Vesuvius and Campi Flegrei, in terms of invaded area and maximum runout. These are the key observables for producing hazard maps of PDC invasion;
2. In Tierz, Sandri, Costa, Sulpizio, et al. (2016) the importance of structural uncertainty (i.e., the uncertainty deriving from all the simplifications of the model itself, or in other words the uncertainty remaining after having run the model using perfectly known boundary conditions and the "best" parameter values Rougier & Beven, 2013) was quantified for the case of Somma-Vesuvius, and it appeared to be much less important than other sources of uncertainty, such as the theoretical and parametric uncertainty, that have been included in our PVHA. In other words, in the case of Somma-Vesuvius at least, different assumptions on model parameters' mutual relationships (theoretical uncertainty) or on the shape of their probability density functions (parametric uncertainty) produced much larger differences in the modeled invaded area or maximum runout, with respect to differences between the best runs of such model and the area and maximum runout measured from PDC deposits at the volcano (see Table 9.2 in Tierz, Sandri, Costa, Zaccarelli, et al., 2016).

A limit in our simulation strategy, in terms of PDC propagation, is that we neglect the presence of the sea in the propagation of PDCs (similarly to Neri et al., 2015). In other words, when a flow reaches the sea, the energy cone model propagates as if there was land, which is obviously a rough approximation: previous works (e.g., Carey et al., 1996; Cordoba, 2007; Dufek et al., 2007) have discussed possible complex and/or transient PDCs-water interactions (e.g., mixture expansion due to sudden vaporization of sea water, enhancing turbulence and diminishing basal friction; loss of denser particles sinking in the water; and entrainment of water, cooling the mixture). These processes are clearly too complex to be captured by the simple linear decay in energy modeled by energy cone. In any case, while the dense basal part of PDCs may lose speed or even sink at the shore, the upper dilute part may propagate over water. This decoupling of dense to dilute parts, and consequent propagation of the latter over the sea surface for tens of kilometers, has been witnessed in historical cases (e.g., Krakatau, 1883; Pompeii 79 AD; Carey et al., 1996; Gurioli et al., 2010). In this view, we highlight that our probability maps include some simulations from Campi Flegrei in which PDCs flow across the Pozzuoli Bay or the Gulf of Napoli and a few simulations from Somma-Vesuvius whose PDCs travel over the sea water of the Gulf of Napoli. As stated above, we are aware that the complexity of the interaction between the sea and these PDCs is far from being captured by the energy cone model: however, these unrealistic simulations represent a very small percentage of the total number of simulations run, and hence, they do not significantly affect the final probability maps.

Another limitation of the energy cone model is that it cannot capture some physical processes relevant for hazard assessment such as PDC channelization (e.g., Tierz, Sandri, Costa, Sulpizio, et al., 2016): this is especially relevant for the dense, basal part of PDCs. For example, we might expect that the probability of PDC invasion computed on the western edge of Mount Somma (where PDCs channelized due to the presence of this barrier might converge, e.g., Esposti Ongaro et al., 2008) represents an underestimation of the true frequency of such PDCs arriving to this area. Future improvements could nonetheless make use of hierarchical modeling (e.g., Selva et al., 2010) taking the present PVHA as the hyper-prior model, updating it with the results from simulations from more sophisticated simulators (e.g., Esposti Ongaro et al., 2008; Patra et al., 2005).

5. Conclusions

In this study, we take a step forward toward a complete PVHA for PDC invasion over the metropolitan area of Napoli, in Southern Italy, accounting for both aleatory variability and epistemic uncertainty. To do so, we introduce some important features in our hazard assessment.

First of all, we consider different (in this case, two) volcanic sources threatening the target area, similarly to the common practice in probabilistic seismic hazard assessment. Even though this may look useless in the case of a volcanic emergency, which is usually (and hopefully) caused by a single source at a time, our PVHA is useful for long-term strategy for risk mitigation, as it is the first step toward a quantitative ranking of (i) the different sources of PDC hazard at a given location and (ii) the different sources of natural risks in the target area.

Second, we introduce a novel approach to quantify the spatially varying epistemic uncertainty associated with the modeling of the area of PDC invasion with the energy cone: up to now, such quantification has been mainly derived from expert judgment (e.g., Neri et al., 2015) or experts' subjective choice (e.g., Sandri et al., 2012, 2014). In particular, we focus on the largest source of epistemic uncertainty previously identified by Tierz, Sandri, Costa, Sulpizio, et al. (2016), that is, the theoretical uncertainty linked to possible correlation patterns between the column collapse height and the flow mobility, which may arise in particular fluid dynamical conditions during the collapse.

Finally, to address the issue of parametric uncertainty (related to the unknown PDF of the model parameters), we propose a final PVHA based on the ensemble of two end-member assumptions on the PDF governing the collapse height: one based on a uniform distribution (describing a situation of maximum ignorance), and one based on an exponential PDF (reflecting the general idea that large column collapse heights are by far less likely than smaller ones, which is a common feature of frequency-size relationships in nature, such as the Gutenberg-Richter law for earthquakes).

To conclude, we underline the importance of these types of probabilistic volcanic hazard assessment as an input to rational decision protocols.

Appendix A: Past Vents (22 ka BP) Explosive Eruptions at Somma-Vesuvius

In this appendix we provide in Table A1 the age, some physical parameters and the vent position estimated for VEI $\geq$ 3 explosive eruptions at Somma-Vesuvius (Italy) during the last 22 ka of volcanic activity, extracted from Cioni et al. (2008).

Table A1
Age, Some Physical Parameters, and Vent Position Estimated for VEI $\geq$ 3 Explosive Eruptions at Somma-Vesuvius (Italy) During the Last 22 ka of Volcanic Activity (After Cioni et al., 2008)

Eruption[a]	Age	TF vol. (km^3)	PDC vol. (km^3)	VEI[b]	"Cioni08-size"	Vent Long. (UTM m)	Vent Lat. (UTM m)	References
Pomici di Base	22 ka Cal	4.4	0.18	5	5	450371	4518947	Santacroce et al. (2008), Cioni et al. (2008), and Gurioli et al. (2010)
Greenish pumice	19 ka Cal	0.5	0.02	4	4	450382	4519688	Santacroce et al. (2008), Cioni et al. (2008), and Gurioli et al. (2010)
Mercato	8.9 ka Cal	1.4	0.23	5	5	451600	4519080	Santacroce et al. (2008), Cioni et al. (2008), and Gurioli et al. (2010)
Avellino	3.9 ka Cal	1.57	1.04	5	5	449420	4518674	Gurioli et al. (2010), Sevink et al. (2011), and Cioni et al. (2000)
AP1	3.5 ka Cal	0.147	–	4	3	449420	4518674	Santacroce et al. (2008), Cioni et al. (2008), and Cioni et al. (2000)
AP2	3.5 ka Cal	0.143	–	4	3	449420	4518674	Santacroce et al. (2008), Cioni et al. (2008), and Cioni et al. (2000)
AP3	2.8 ka Cal	0.15	–	4	1	451600	4519080	Santacroce et al. (2008), Cioni et al. (2008), and Cioni et al. (2000)

Table A1 *(continued)*

Eruption[a]	Age	TF vol. (km^3)	PDC vol. (km^3)	VEI[b]	"Cioni08-size"	Vent Long. (UTM m)	Vent Lat. (UTM m)	References
AP4	–	0.122	–	4	1.5[c]	451600	4519080	Cioni et al. (2008) and Cioni et al. (2000)
AP5	–	0.084	–	3	1.5[c]	451600	4519080	Cioni et al. (2008) and Cioni et al. (2000)
AP6	216–217 BC	–	–	1	2	451600	4519080	Santacroce et al. (2008) and Cioni et al. (2000)
Pompeii	79 AD	2.9	0.83	5	5	452132	4518798	Gurioli et al. (2010) and Cioni et al. (2003)
Santa Maria cycle	172 AD[d]	0.15	–	4	1.5[c]	452132	4518798	Cioni et al. (2008) and Johnston-Lavis (1884)
Pollena	472 AD	1.38	0.39	5	4	450769	4520035	Cioni et al. (2008), Gurioli et al. (2010), and Sulpizio et al. (2005)
AS1	512 AD	0.025	–	3	3	451600	4519080	Andronico et al. (1995) and Cioni et al. (2011)
AS2	540 AD	0.04	–	3	2	451600	4519080	Santacroce et al. (2008) and Cioni et al. (2008)
AS3	640 AD	0.12	–	4	2	451600	4519080	Santacroce et al. (2008) and Cioni et al. (2008)
AS4	790 AD	0.01	–	3	2	451600	4519080	Santacroce et al. (2008) and Cioni et al. (2008)
AS5	1410 AD	–	–	1	2	451600	4519080	Santacroce et al. (2008)
AD1631	1631 AD	1.09	0.2	5	4	451600	4519080	Cioni et al. (2008), Gurioli et al. (2010), and Rolandi et al. (1993)
SO1	1660 AD	–	–	1	1	451600	4519080	Cioni et al. (2008) and Arrighi et al. (2001)
SO2	1682 AD	0.0056	–	2	2	451600	4519080	Cioni et al. (2008) and Arrighi et al. (2001)
SAD1	1707 AD	0.0013	–	2	2	451600	4519080	Cioni et al. (2008) and Arrighi et al. (2001)
FdL	1723 AD	0.008	–	2	2	451600	4519080	Cioni et al. (2008) and Arrighi et al. (2001)
T1	1730 AD	0.0012	–	2	2	451600	4519080	Cioni et al. (2008) and Arrighi et al. (2001)
OTV	1779 AD	0.0061	–	2	2	451600	4519080	Cioni et al. (2008) and Arrighi et al. (2001)
CFM	1794 AD	–	–	1	1	451600	4519080	Cioni et al. (2008)
AD1822	1822 AD	0.038	–	3	2	451600	4519080	Cioni et al. (2008) and Arrighi et al. (2001)
AD1906	1906 AD	0.071	–	3	2	451600	4519080	Cioni et al. (2008) and Arrighi et al. (2001)
AD1944	1944 AD	0.066	$5.7 \cdot 10^{-3}$	3	2	451600	4519080	Cioni et al. (2008), Pesce and Rolandi (1994), and Hazlett et al. (1991)

Note. Only eruptions for which the position of the eruptive vent is relatively well constrained are included. The term "*Cioni08-size*" refers to the classification given by Cioni et al. (2008): 1 = ash emission (AE), 2 = Violent Strombolian (VS), 3 = Sub-Plinian II (SPl2), 4 = Sub-Plinian I (SPl1), 5 = Plinian (Pl). UTM coordinates correspond to zone 33N.

[a]Abbreviations of the eruption names are taken from Cioni et al. (2008). [b]VEI size is calculated from the total erupted volume, in terms of tephra fallout (TF) and pyroclastic density currents (PDC) volume. [c]A value of 1.5 indicates that Cioni et al. (2008) classified the eruption as AE-VS. [d]This age denotes the beginning of the eruptive cycle.

Appendix B: Modeling Procedure

B1. Definition of the Two End-Member Probability Distributions for H_0

B1.1. Truncated Exponential Distribution

In this case we adopt the same paradigm as in Tierz, Sandri, Costa, Sulpizio, et al. (2016) and Tierz, Sandri, Costa, Zaccarelli, et al. (2016). For each eruption size class, we first account for the total column heights derived from eruption column simulations at Somma-Vesuvius and Campi Flegrei in Sandri et al. (2016). In that work, column height (H_T) values were calculated from mass eruption rates through the fourth-power relationship by Mastin et al. (2009), in turn computed after having sampled, from proper PDFs set for the two volcanoes, values of total erupted mass and eruption duration. Second, we assume that the top of the gas thrust region top is roughly estimated as 10% of the total height of the eruption column (Wilson et al., 1978). In this way, the parameter λ defining the truncated exponential PDF H_0 is inferred by assuming that the top of the gas thrust region marks the 95th percentile of the corresponding nontruncated exponential PDF. The obtained Exponential PDFs are then truncated and renormalized between $H_{0_{min}} = 20$ m and $H_{0_{max}} = 0.1H_T$.

In our simulation scheme, for each volcano and eruptive size class, we sample 1,000 H_T values from Sandri et al. (2016). For each of these, we retrieve a λ value and so a truncated exponential distribution, from which we sample 10 values of H_0. Thus, we end up with 10,000 H_0 values for each volcano and eruptive size class. Correspondingly, we sample 10,000 ϕ values given the volcano and eruptive size class. Finally, we run the energy cone model 10,000 times (one for each pair (H_0, ϕ)) for every given possible volcano (2), vent position (441 and 460 for Somma-Vesuvius and Campi Flegrei, respectively) and size class (3 for each volcano), totalling

$10^4 \times 441 \times 3$ and $10^4 \times 460 \times 3$ simulations for Somma-Vesuvius and Campi Flegrei, respectively. Such a large number of simulations is necessary to sample correctly the tail of the exponential PDF adopted. In order to lower the computational time, in the case of the 392 lateral vents at Vesuvius (having very low probability) we only run 1,000 simulations, so in the end we run energy cone model $10^4 \times 49 \times 3 + 10^3 \times 392 \times 3$ times (approximately $2.5 \cdot 10^6$ times). For Campi Flegrei we run 10^4 simulations for each eruptive vent and eruption size (approximately $1.4 \cdot 10^7$ times).

B1.2. Uniform Distribution

In this case, we again account for the total column heights derived from eruption column simulations at Somma-Vesuvius and Campi Flegrei in Sandri et al. (2016) and assume that the top of the gas thrust region top is roughly estimated as 10% of the total height of the eruption column (Wilson et al., 1978). In this way, the uniform distribution is set between $H_{0_{min}}$=20 m and $H_{0_{max}} = 0.1H_T$.

In our simulation scheme, for each volcano and eruptive size class, we again sample 1,000 H_T values from Sandri et al. (2016) and define 1,000 uniform distributions. From each one of these, we sample one value of H_0. Thus, we end up with 1,000 H_0 values for each volcano and eruptive size class. Correspondingly, we sample 1,000 ϕ values given the volcano and eruptive size class. Finally, we run energy cone model 1,000 times (one for each pair (H_0, ϕ)) for every given possible volcano, vent position and size class. In the case of uniform distributions the number of samples can be lower as it is not too difficult to effectively sample the whole range of possible values of H_0 (the uniform distribution has no real "tail").

B2. Energy Cone Simulations

The energy cone model is implemented on MATLAB (MathWorks, 2012) and run on a 40-m DEM using computing facilities at the Center for Computational Research of the University at Buffalo, NY, USA. For Somma-Vesuvius, Tierz, Sandri, Costa, Sulpizio, et al. (2016) demonstrated that the use of a 40-m DEM does not alter the output of the energy cone simulations considerably, with respect to other sources of uncertainty, compared to a finer DEM (the importance of the theoretical uncertainty, i.e., direct or inverse relationship between H_0 and ϕ, is one to two order of magnitudes larger). For Campi Flegrei we do not have such a systematic quantification for all the sources of uncertainty. We are aware that in the case of calderas, the absence of a predominant topographic structure could give a more relevant role to DEM resolution, compared to other sources of uncertainty. However, given the overwhelming difference in the importance of theoretical uncertainty with respect to input uncertainty (i.e., DEM resolution) in the case of Somma-Vesuvius, we assume that for Campi Flegrei the usage of a 40-m DEM influences the results to a lesser extent than theoretical uncertainty does.

The output of the simulations are then interpolated on a 100-m grid for the PVHA, keeping the maximum value of frequency of PDC arrival after the interpolation. This reduction is necessary to keep the computational time of BET_VH model acceptable.

The final domain of PVHA is thus on a 100-m grid with lower left and upper right corners respectively at (402575,4486891) and (483375,4546091) UTM (zone 33).

Appendix C: Results Obtained by Using Other Evaluation for the Spatial Probability of Vent Opening

In this study, we made use of the spatial probability of vent opening for Campi Flegrei by Selva et al. (2012) and we performed a new one for Somma-Vesuvius (section 2.1.1).

In Figure C1 we show the difference in the probability of PDC arrival, given the occurrence of an eruption of any size and from any vent, when using other maps for the spatial probability of vent opening. In particular, in Figures C1a and C1b we show (for the two end-member PDF for the collapse height) the difference in the above conditional probability when using the map recently proposed for Somma-Vesuvius by Tadini et al. (2017) with respect to the map used in this study. To compute such difference map, we have regridded the map by Tadini et al. (2017) (their Figure 8) on our coarser grid for Node 4 (section 2.1.1). In particular, to any given grid cell in our vents' grid, we assign the sum of the probability values of all their grid points falling within our given cell. We see from Figures C1a and C1b that using the map by Tadini et al. (2017) results in conditional probability values which are systematically and significantly lower (more than 30% in some areas) than using the map proposed in the present paper. This is mostly due to the fact that their vent map is almost a uniform map over the summit caldera, and this results in a "dissipating" effect similar to the one we observe

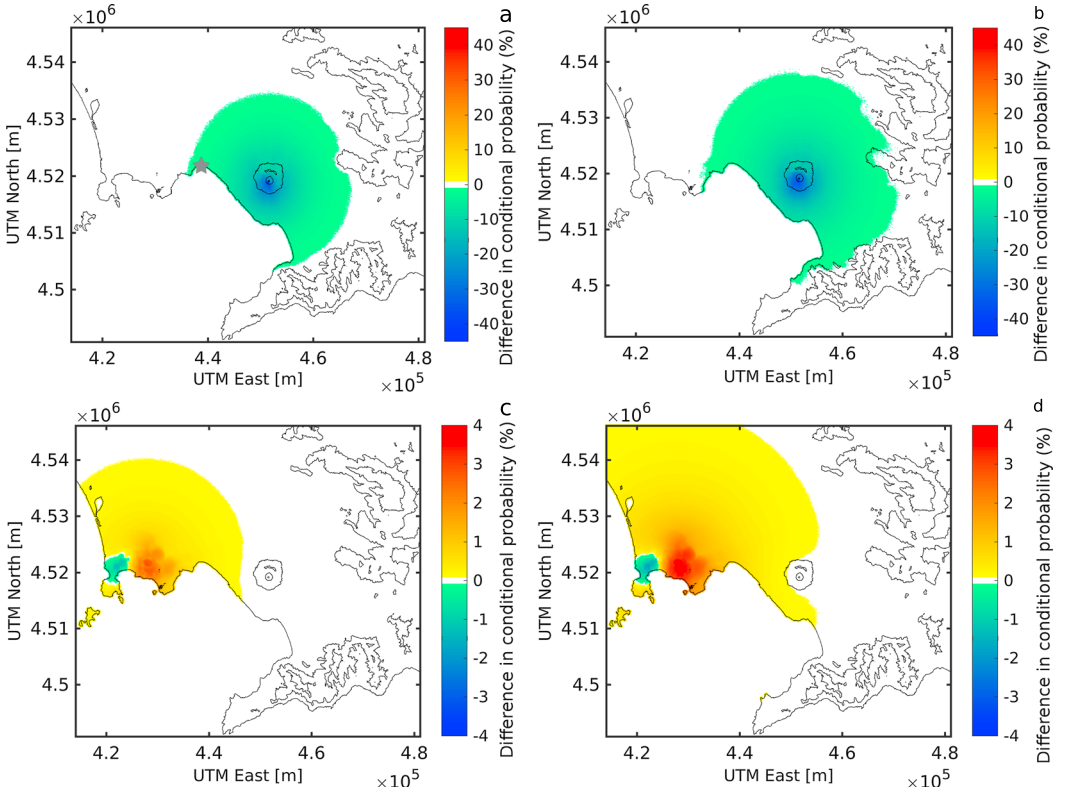

Figure C1. Differences in the probability of pyroclastic density currents (PDF) arrival, given the occurrence of an eruption of any size and from any vent, when using other maps for the spatial probability of vent opening. (a) (exponential PDF for the collapse height) and (b) (uniform PDF for the collapse height) show the difference in the above conditional probability when using the map recently proposed for Somma-Vesuvius by Tadini et al. (2017) with respect to the map used in this study. Negative values mean that the final Probabilistic Volcanic Hazard Assessment (PVHA) is underestimated when using the vent map by Tadini et al. (2017), with respect to the one proposed here. (c) (exponential PDF for the collapse height) and (d) (uniform PDF for the collapse height) show the difference in the above conditional probability when using the map proposed for Campi Flegrei by Bevilacqua et al. (2015) with respect to the map used in this study based on Selva et al. (2012). Positive/negative values mean that the final PVHA is overestimated/underestimated, respectively, when using the vent map by Bevilacqua et al. (2015), with respect to the one proposed here. Note the difference in the color scale between Somma-Vesuvius panels (a, b) and Campi Flegrei panels (c, d).

at Campi Flegrei. We believe that these results justify the use of our map here proposed, as the final results are much more conservatives in terms of PVHA.

Analogously, for Campi Flegrei, in Figure C1c,d we show (for the two end-member PDF for the collapse height) the difference in the probability of PDC arrival, given the occurrence of an eruption of any size and from any vent,the conditional probability when using the map recently proposed by Bevilacqua et al. (2015) with respect to the map used in this study. Since the map by Bevilacqua et al. (2015) is very similar to the one by Selva et al. (2012) used in this study (both in terms of evidence based to build it, and in the resulting numerical values), we see that in this case the differences in the conditional probability are limited to a few percent points (maximum 4%), and do not show a systematic under or over estimation when using either one of the two. In turn, the use of the two maps in the probability of PDC arrival in 50 years does not change significantly the results, and the differences are within our final confidence bounds mentioned above.

Appendix D: Comparisons With Previous PDC Hazard Assessments at Somma-Vesuvius and Campi Flegrei

D1. Somma-Vesuvius

A qualitative comparison of our maps for the probability of PDC invasion in the next 50 years can be made with the PDC hazard assessment of Gurioli et al. (2010) (based on past PDC deposits) and Neri et al. (2008) (based on expert elicitation and numerical modeling of PDCs). A comparison of Figure 2 with the most recent

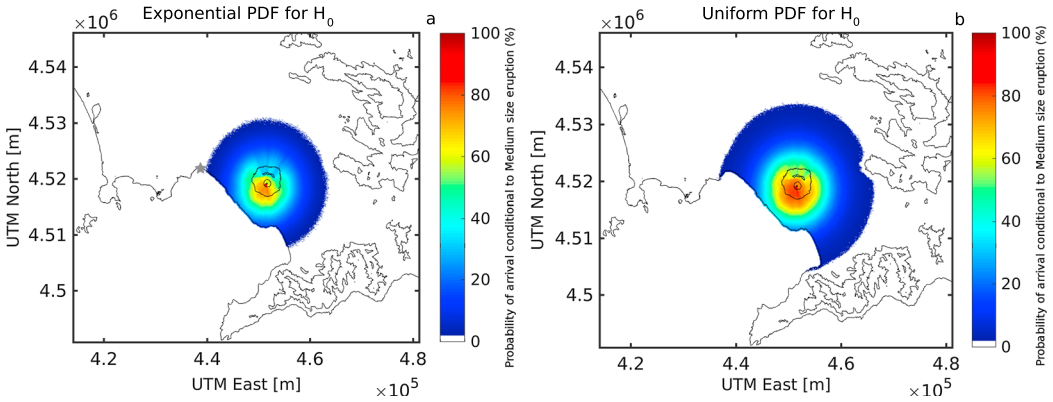

Figure D1. Maps used to qualitatively compare our results with those by Neri et al. (2008) at Somma-Vesuvius. (a) and (b) show, respectively, the expected probability of pyroclastic density currents (PDC) arrival, given an eruption of medium size from the central crater (in %), according to the exponential and uniform models for H_0 presented in this paper. To be compared with Figure 9 by Neri et al. (2008). Gray star points to the downtown of Napoli.

frequency map of PDC deposits around Somma-Vesuvius (Figure 6 in Gurioli et al., 2010) informs that the isoline enclosing the area having experienced at least two PDC arrivals in the last 22 ka coincides approximately with the one with a mean probability of at least 1% in 50 years (Figure 2c). By using our mean probability value, and assuming a Binomial PDF to model the arrival of PDCs (in n time windows) at a given grid point, the probability of observing at least two PDC arrivals in that area in 440 time windows of 50 years each (i.e., 22 ka in total) is about 99%. Accounting for uncertainties in both our model and field data (e.g., possible incompleteness in the field observations), this crude comparison highlights that our mean probability values seem statistically consistent with the observed frequency of PDCs reported by Gurioli et al. (2010).

On the other hand, if we compare our ensemble probabilities of PDC arrival (for any size and any vent, Figure (2)) with the 90% confidence interval provided by Neri et al. (2008) (their Figure 9) for different sectors around Somma-Vesuvius (given an eruption of medium size or "Sub-Plinian I," as defined by Cioni et al., 2008), we observe that the spatial pattern is similar: both the study of Neri et al. (2008) and ours confirm the importance of Mount Somma in hindering PDC propagation toward the north. In terms of probability values, the comparison with Figure 2 is difficult because the study by Neri et al. (2008) shows elicited probabilities conditional upon the occurrence of a medium size eruption from the main crater, while we show absolute probabilities for the next 50 years from any kind of eruption (any size and vent). Nevertheless, our mean probability of PDC invasion beyond Mount Somma is between 4 and 6%, which is about half the probability on the opposite southern flank, at a similar distance (between 10 and 12%, Figures 2c and 2d). This spatial pattern is in agreement with the one for the elicited values by Neri et al. (2008) (e.g., median probabilities of PDC invasion are around 90–95% over the southern, western, and eastern flanks of the volcano, but only 45% on the northern flank, beyond Mount Somma).

If we compare the results presented by Neri et al. (2008) with the probabilities of PDC arrival, given a medium-size eruption from the central crater, computed from our two end-member models for the collapse height (Figure D1), we note that the hazard assessment of Neri et al. (2008) is somehow intermediate between the two end-member models. Thus, the 50% probability points of the exponential model (Figure D1a) show a strong influence of the Mount Somma in hindering PDC propagation toward the north, similar to what proposed by Neri et al. (2008) in their Figure 9, but our maximum runouts are a bit shorter than those presented by Neri et al. (2008) for the same probability of PDC arrival (green lines in their Figure 9). In contrast, the 50% probability points of the uniform model (Figure D1b) display maximum runouts that are closer to the ones given by Neri et al. (2008) over the southern, western, and eastern flanks of the volcano. On the northern flank, the 50% probability points obtained with the uniform model seem not to be influenced by the presence of Mount Somma, which is in relative disagreement with the hazard assessment of Neri et al. (2008). Nevertheless, it could be argued that independently of the proportion of PDCs that are able to overcome the topographic barrier of Mount Somma (i.e., frequency of PDC arrival beyond it), the ones that actually propagate further northward might reach maximum runouts that are not very different from the ones recorded over the southern flank (e.g., Baxter et al., 1998; Todesco et al., 2002). Therefore, the probabilities of PDC

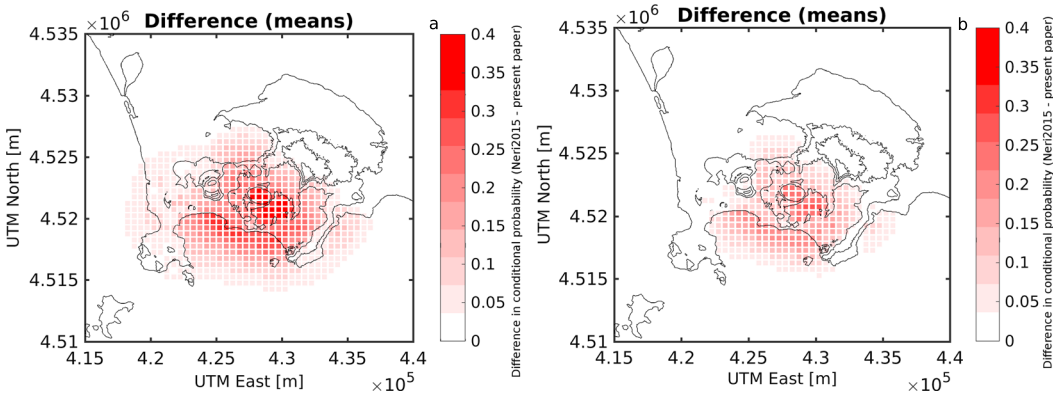

Figure D2. Differences in the mean probability of pyroclastic density currents arrival, conditional upon the occurrence of an eruption from an inland vent at the Campi Flegrei caldera, computed by Neri et al. (2015) minus those computed in this study. Positive values (red) indicate that the probability of pyroclastic density currents arrival is greater in Neri et al. (2015). The differences are expressed in the unit interval: [0, 1]. (a) and (b) are respectively for the exponential and uniform models for the collapse height.

arrival for large (infrequent) PDCs are less constrained by the presence Mount Somma (Tierz, Sandri, Costa, Sulpizio, et al., 2016).

D2. Campi Flegrei

In the case of Campi Flegrei, we compare some of our partial results with the ones obtained by Neri et al. (2015). In particular, in Figure D2, we show the difference between the probability of invasion of PDCs, conditional upon the occurrence of an eruption of any size from an inland vent of Campi Flegrei caldera, obtained by Neri et al. (2015) and by our hazard assessment. We show such difference for both end-member assumptions on the PDF for the collapse height (exponential and uniform).

The differences with Neri et al. (2015) are as follows:

1. always positive, implying that our method produces, systematically, either comparable or smaller probabilities of PDC invasion;
2. particularly large over the Astroni crater and the Agnano plain (absolute values are up to ~40% and ~30% for the exponential and uniform H_0 models, respectively);
3. less significant along elevated areas (e.g., Posillipo hill) and the western sector of the caldera, especially in the case of the uniform model for H_0.

Acknowledgments

This work was partially supported by the EU FP7 project Numerical, Experimental, and stochastic Modelling of vOlcanic processes and Hazard (NEMOH, grant agreement 289976), EU FP7 project MEDiterrenean SUpersite Volcanoes (MED-SUV, grant agreement 308665), and the "Futuro in Ricerca 2008 FIRB" *ByMuR* Project (RBFR0880SR) funded by MIUR (the Italian Ministry of Education, University and Research), This work benefited from the agreement between Istituto Nazionale di Geofisica e Vulcanologia (INGV) and the Italian Presidenza del Consiglio dei Ministri, Dipartimento della Protezione Civile (DPC). This paper does not necessarily represent DPC official opinion and policies. Background roadmap, terrain, or satellite images in all the pictures, when present, are automatically downloaded from Google Maps. Some results shown here were obtained through computational resources provided by the Center for Computational Research, University at Buffalo, NY, USA. We sincerely thank Giuseppe Vilardo (Laboratory of Geomatics and Cartography, INGV-OV) for providing some DEM products and Jacopo Selva, Roberto Sulpizio, Lucia Zaccarelli, and Mauro Antonio Di Vito for useful discussions concerning some of the topics treated in the manuscript. We are also grateful to the Associate Editor, Piero Dellino and two anonymous reviewers for greatly improving our first version of the manuscript through their careful reading and commenting. The data supporting the conclusions are shown in the figures presented. The spatial distribution of vent opening at Somma-Vesuvius is available in the supporting information. On request, the authors can provide output MATLAB files containing the results. L. S., P. T., A. C., and W. M. conceived the study, L. S. and P. T. analyzed the results and prepared the figures, L. S. wrote the paper with input from the other authors, P. T. and L. S. provided the model parameters, and P. T. carried out the energy cone simulations. L. S. performed the BET_VH modeling. All authors reviewed the manuscript.

References

Alberico, I., Petrosino, P., & Lirer, L. (2011). Volcanic hazard and risk assessment in a multi-source volcanic area: The example of Napoli city (Southern Italy). *Natural Hazards and Earth System Sciences*, *11*, 1057–1070. https://doi.org/10.5194/nhess-11-1057-2011

Andronico, D., Calderoni, G., Cioni, R., Sbrana, A., Sulpizio, R., & Santacroce, R. (1995). Geological map of Somma-Vesuvius volcano. *Periodico di Mineralogia*, *64*(1-2), 77–78.

Andronico, D., & Cioni, R. (2002). Contrasting styles of Mount Visuvius activity in the period between the Avellino and Pompeii Plinian eruptions, and some implications for assessment of future hazards. *Bulletin of Volcanology*, *64*(6), 372–391.

Arrighi, S., Principe, C., & Rosi, M. (2001). Violent strombolian and subplinian eruptions at Vesuvius during post-1631 activity. *Bulletin of Volcanology*, *63*(2-3), 126–150.

Auker, M. R., Sparks, R. S. J., Siebert, L., Crosweller, H. S., & Ewert, J. (2013). A statistical analysis of the global historical volcanic fatalities record. *Journal of Applied Volcanology*, *2*, 2. https: //doi.org/10.1186/2191-5040-2-2

Baxter, P., Neri, A., & Todesco, M. (1998). Physical modelling and human survival in pyroclastic flows. *Natural Hazards*, *17*(2), 163–176.

Bayarri, M., Berger, J., Calder, E. S., Dalbey, K., Lunagomez, S., Patra, A. K., et al. (2009). Using statistical and computer models to quantify volcanic hazards. *Technometrics*, *51*(4), 402–413.

Bebbington, M. S., & Cronin, S. J. (2010). Spatio-temporal hazard estimation in the Auckland Volcanic Field, New Zealand, with a new event-order model. *Bulletin of Volcanology*, *73*(1), 55–72.

Best, M. J., Abramowitz, G., Johnson, H., Pitman, A., Balsamo, G., Boone, A., et al. (2015). The plumbing of land surface models: Benchmarking model performance. *Journal of Hydrometeorology*, *16*(3), 1425–1442.

Bevilacqua, A., Bursik, M., Patra, A., Pitman, E. B., & Till, R. (2017). Bayesian construction of a long-term vent opening probability map in the Long Valley volcanic region (CA, USA). *Statistics in Volcanology*, *3*, 1–36. https://doi.org/10.5038/2163-338X.3.1

Bevilacqua, A., Flandoli, F., Neri, A., Isaia, R., & Vitale, S. (2016). Temporal models for the episodic volcanism of Campi Flegrei caldera (Italy) with uncertainty quantification. *Journal of Geophysical Research: Solid Earth*, *121*, 7821–7845. https://doi.org/10.1002/2016JB013171

Bevilacqua, A., Isaia, R., Neri, A., Vitale, S., Aspinall, W., & Bisson, M. (2015). Quantifying volcanic hazard at Campi Flegrei caldera (Italy) with uncertainty assessment: 1. Vent opening maps. *Journal of Geophysical Research: Solid Earth*, *120*, 2309–2329. https://doi.org/10.1002/2014JB011775

Branney, M. J., & Kokelaar, B. P. (2002). *Pyroclastic density currents and the dedimentation of ignimbrites*. London: Geological Society.
Carey, S., Sigurdsson, H., Mandeville, C., & Bronto, S. (1996). Pyroclastic flows and surges over water: An example from the 1883 Krakatau eruption. *Bulletin of Volcanology*, *57*, 493–511.
Charbonnier, S. J., & Gertisser, R. (2012). Evaluation of geophysical mass flow models using the 2006 block-and-ash flows of Merapi Volcano, Java, Indonesia: Towards a short-term hazard assessment tool. *Journal of Volcanology and Geothermal Research*, *231*, 87–108.
Cioni, R., Bertagnini, A., Andronico, D., Cole, P., & Mundula, F. (2011). The 512 AD eruption of Vesuvius: Complex dynamics of a small scale Subplinian event. *Bulletin of Volcanology*, *73*(7), 789–810.
Cioni, R., Bertagnini, A., Santacroce, R., & Andronico, D. (2008). Explosive activity and eruption scenarios at Somma-Vesuvius (Italy): Towards a new classification scheme. *Journal of Volcanology and Geothermal Research*, *178*, 331–346.
Cioni, R., Levi, S., & Sulpizio, R. (2000). Apulian Bronze Age pottery as a long-distance indicator of the Avellino Pumice eruption (Vesuvius, Italy). *Special Publications*, *171*(1), 159–177.
Cioni, R., Santacroce, R., & Sbrana, A. (1999). Pyroclastic deposits as a guide for reconstructing the multi-stage evolution of the Somma-Vesuvius caldera. *Bulletin of Volcanology*, *61*, 207–222.
Cioni, R., Sulpizio, R., & Garruccio, N. (2003). Variability of the eruption dynamics during a Subplinian event: The Greenish Pumice eruption of Somma–Vesuvius (Italy). *Journal of Volcanology and Geothermal Research*, *124*(1), 89–114.
Clarke, A., Voight, B., Neri, A., & Macedonio, G. (2002). Transient dynamics of vulcanian explosions and column collapse. *Nature*, *415*(6874), 897–901.
Cordoba, G. (2007). Dilute particle-laden currents: Dynamics and deposit patterns (PhD Thesis), University of Bristol.
Dalbey, K., Patra, A. K., Pitman, E. B., Bursik, M. I., & Sheridan, M. F. (2008). Input uncertainty propagation methods and hazard mapping of geophysical mass flows. *Journal of Geophysical Research*, *113*, B05203. https://doi.org/10.1029/2006JB004471
Deino, A. L., Orsi, G., de Vita, S., & Piochi, M. (2004). The age of the neapolitan yellow tuff caldera-forming eruption (Campi Flegrei caldera–Italy) assessed by $^{40}Ar/^{39}Ar$ dating method. *Journal of Volcanology and Geothermal Research*, *133*(1), 157–170.
Dellino, P., Mele, D., Sulpizio, R., La Volpe, L., & Braia, G. (2008). A method for the calculation of the impact parameters of dilute pyroclastic density currents based on deposit particle characteristics. *Journal of Geophysical Research*, *113*, B07206. https://doi.org/10.1029/2007JB005365
Doyle, E., Hogg, A., Mader, H., & Sparks, R. S. J. (2010). A two-layer model for the evolution and propagation of dense and dilute regions of pyroclastic currents. *Journal of Volcanology and Geothermal Research*, *190*, 365–378.
Druitt, T. (1998). Pyroclastic density currents. *Special Publications*, *145*(1), 145–182.
Dufek, J., Manga, M., & Staedter, M. (2007). Littoral blasts: Pumice-water heat transfer and the conditions for steam explosions when pyroclastic flows enter the ocean. *Journal of Geophysical Research*, *112*, B11201. https://doi.org/10.1029/2006JB004910
Esposti Ongaro, T., Neri, A., Menconi, G., de' Michieli Vitturi, M., Marianelli, P., Cavazzoni, C., et al. (2008). Transient 3D numerical simulations of column collapse and pyroclastic density current scenarios at Vesuvius. *Journal of Volcanology and Geothermal Research*, *178*, 378–396.
Fedele, F. G., Giaccio, B., Isaia, R., & Orsi, G. (2003). The campanian ignimbrite eruption, Heinrich Event 4, and Palaeolithic change in Europe: A high-resolution investigation. In A. Robock & C. Oppenheimer (Eds.), *Volcanism and the Earth's atmosphere* (Vol. 139, pp. 301–325). Washington, DC: American Geophysical Monograph.
Gelman, A., Carlin, J. B., Stern, H. S., Dunson, D. B., Vehtari, A., & Rubin, D. B. (2013). *Bayesian data analysis* (3rd ed., p. 675). London: Chapman and Hall/CRC.
Gurioli, L., Sulpizio, R., Cioni, R., Sbrana, A., Santacroce, R., Luperini, W., & Andronico, D. (2010). Pyroclastic flow hazard assessment at Somma–Vesuvius based on the geological record. *Bulletin of Volcanology*, *72*, 1021–1038.
Hayashi, J., & Self, S. (1992). A comparison of pyroclastic flow and debris avalanche mobility. *Journal of Geophysical Research*, *97*(B6), 9063–9071.
Hazlett, R., Buesch, D., Anderson, J., Elan, R., & Scandone, R. (1991). Geology, failure conditions, and implications of seismogenic avalanches of the 1944 eruption at Vesuvius, Italy. *Journal of Volcanology and Geothermal Research*, *47*, 249–264.
Huppert, H. E., & Simpson, J. E. (1980). The slumping of gravity currents. *Journal of Fluid Mechanics*, *99*(4), 785–799. https://doi.org/10.1017/S0022112080000894
Jenkins, S., Magill, C., McAneney, J., & Blong, R. (2012). Regional ashfall hazard I: A probabilistic assessment methodology. *Bulletin of Volcanology*, *74*, 1699–1712. https://doi.org/10.1007/ s00445-012-0627-8
Johnston-Lavis, H. J. (1884). The geology of Monte Somma and Vesuvius, being a study in vulcanology. *Quarterly Journal of the Geological Society*, *40*(1-4), 35–119.
Jordan, T., Marzocchi, W., Michael, A., & Gerstenberger, M. (2014). Operational earthquake forecasting can enhance earthquake preparedness. *Seismological Research Letters*, *85*(5), 955–959. https://doi.org/10.1785/0220140143
Kelfoun, K., & Druitt, T. (2005). Numerical modelling of the emplacement of the 7500 BP Socompa rock avalanche, Chile. *Journal of Geophysical Research*, *110*, B12202. https://doi.org/10.1029/2005JB003758
Lindsay, J., Marzocchi, W., Jolly, G., Constantinescu, R., Selva, J., & Sandri, L. (2010). Towards real-time eruption forecasting in the Auckland Volcanic Field: Application of BET _ EF during the New Zealand National Disaster Exercise "Ruaumoko". *Bulletin of Volcanology*, *72*, 185–204. https://doi.org/10.1007/ s00445-009-0311-9
Lirer, L., Petrosino, P., & Alberico, I. (2010). Hazard and risk assessment in a complex multi-source volcanic area: The example of the Campania Region, Italy. *Bulletin of Volcanology*, *72*(4), 411–429. https: //doi.org/10.1007/s00445-009-0334-2
Malin, M. C., & Sheridan, M. F. (1982). Computer-assisted mapping of pyroclastic surges. *Science*, *217*, 637–640.
Martin, A. J., Umeda, K., Connor, C. B., Weller, J. N., Zhao, D., & Takahashi, M. (2004). Modeling long-term volcanic hazards through Bayesian inference: An example from the Tohoku volcanic arc, Japan. *Journal of Geophysical Research*, *109*, B10208. https://doi.org/10.1029/2004JB003201
Marzocchi, W., & Jordan, T. (2014). Testing for ontological errors in probabilistic forecasting models of natural systems. *Proceedings of National Academy of Sciences*, *111*(33), 11973–11978.
Marzocchi, W., Sandri, L., Gasparini, P., Newhall, C. G., & Boschi, E. (2004). Quantifying probabilities of volcanic events: The example of volcanic hazard at Mount Vesuvius. *Journal of Geophysical Research*, *109*, B11201. https://doi.org/10.1029/2004JB003155
Marzocchi, W., Sandri, L., & Selva, J. (2008a). BET_EF: A probabilistic tool for long- and short-term eruption forecasting. *Bulletin of Volcanology*, *70*, 623–632. https://doi.org/10.1007/ s00445-007-0157-y
Marzocchi, W., Sandri, L., & Selva, J. (2008b). Probability estimation at the nodes: General aspects. *Bulletin of Volcanology-Electronic Supplementary Material*, 1–20.
Marzocchi, W., Sandri, L., & Selva, J. (2010). BET_VH: A probabilistic tool for long-term volcanic hazard assessment. *Bulletin of Volcanology*, *72*(6), 705–716. https://doi.org/10.1007/s00445-010-0357-8

Marzocchi, W., & Woo, G. (2007). Probabilistic eruption forecasting and the call for an evacuation. *Geophysical Research Letters*, *34*, L22310. https://doi.org/10.1029/2007GL031922

Marzocchi, W., & Woo, G. (2009). Principles of volcanic risk metrics: Theory and the case study of Mount Vesuvius and Campi Flegrei, Italy. *Journal of Geophysical Research*, *114*, B03213. https://doi.org/10.1029/2008JB005908

Mastin, L. G., Guffanti, M., Servranckx, R., Webley, P., Barsotti, S., Dean, K., et al. (2009). A multidisciplinary effort to assign realistic source parameters to models of volcanic ash-cloud transport and dispersion during eruptions. *Journal of Volcanology and Geothermal Research*, *186*, 10–21.

Mastin, L. G., & Witter, J. B. (2000). The hazards of eruptions through lakes and seawater. *Journal of Volcanology and Geothermal Research*, *97*, 195–214.

Neri, A., Aspinall, W. P., Cioni, R., Bertagnini, A., Baxter, P. J., Zuccaro, G., et al. (2008). Developing an Event Tree for probabilistic hazard and risk assessment at Vesuvius. *Journal of Volcanology and Geothermal Research*, *178*(3), 397–415.

Neri, A., Bevilacqua, A., Esposti Ongaro, T., Isaia, R., Aspinall, W. P., Bisson, M., et al. (2015). Quantifying volcanic hazard at Campi Flegrei caldera (Italy) with uncertainty assessment: 2. Pyroclastic density current invasion maps. *Journal of Geophysical Research: Solid Earth*, *120*, 2330–2349. https://doi.org/10.1002/2014JB011776

Newhall, C. G., & Hoblitt, R. P. (2002). Constructing event trees for volcanic crises. *Bulletin of Volcanology*, *64*, 3–20. https://doi.org/10.1007/s004450100173

Ogburn, S. E. (2012). FlowDat: VHub mass flow database. Retrieved from https://vhub.org/resources/2076

Ogburn, S. E., Calder, E. S., Cole, P. D., & Stinton, A. J. (2014). The effect of topography on ash-cloud surge generation and propagation. *Geological Society, London, Memoirs*, *39*(1), 179–194.

Ongaro Esposti, T., Orsucci, S., & Cornolti, F. (2016). A fast, calibrated model for pyroclastic density currents kinematics and hazard. *Journal of Volcanology and Geothermal Research*, *327*, 257–272.

Oramas-Dorta, D., Cole, P. D., Wadge, G., Alvarado, G. E., & Soto, G. J. (2012). Pyroclastic flow hazard at Arenal volcano, Costa Rica: Scenarios and assessment. *Journal of Volcanology and Geothermal Research*, *247*, 74–92.

Orsi, G., Di Vito, M. A., & Isaia, R. (2004). Volcanic hazard assessment at the restless Campi Flegrei caldera. *Bulletin of Volcanology*, *66*, 514–530. https://doi.org/10.1007/s00445-003-0336-4

Orsi, G., Di Vito, M. A., Selva, J., & Marzocchi, W. (2009). Long-term forecast of eruption style and size at Campi Flegrei caldera (Italy). *Earth and Planetary Science Letters*, *287*, 265–276. https://doi.org/10.1016/j.epsl.2009.08.013

Patra, A. K., Bauer, A., Nichita, C., Pitman, E. B., Sheridan, M. F., Bursik, M., et al. (2005). Parallel adaptive numerical simulation of dry avalanches over natural terrain. *Journal of Volcanology and Geothermal Research*, *139*, 1–21.

Pesce, A., & Rolandi, G. (1994). Vesuvio 1944. L-ultima eruzione. S. Sebastiano al Vesuvio, Magma–FLM Napoli.

Pyle, D. (2000). Sizes of volcanic eruptions. In H. Sigurdsson, et al. (Eds.), *Encyclopedia of volcanoes*. London: Academic Press.

Rolandi, G., Barrella, A., & Borrelli, A. (1993). The 1631 eruption of Vesuvius. *Journal of Volcanology and Geothermal Research*, *58*(1), 183–201.

Rougier, J., & Beven, K. (2013). Model limitations: The sources and implications of epistemic uncertainty. In J. Rougier & K. Beven (Eds.), *Risk and uncertainty assessment for natural hazards* (pp. 40–63). Cambridge, UK: Cambridge University Press.

Rougier, S. R. J., andSparks, J, & Cashman, K. V. (2016). Global recording rates for large eruptions. *Journal of Applied Volcanology*, *5*(1), 11.

Salt, J. D. (2008). The seven habits of highly defective simulation projects. *Journal of Simulation*, *2*, 155–161.

Sandri, L., Costa, A., Selva, J., Tonini, R., Macedonio, G., Folch, A., & Sulpizio, R. (2016). Beyond eruptive scenarios: Assessing tephra fallout hazard from Neapolitan volcanoes. *Scientific Reports*, *6*, 24271. https://doi.org/10.1038/srep24271

Sandri, L., Jolly, G., Lindsay, J. M., Howe, T., & Marzocchi, W. (2012). Combining long- and short-term probabilistic volcanic hazard assessment with cost-benefit analysis to support decision making in a volcanic crisis from the Auckland Volcanic Field, New Zealand. *Bulletin of Volcanology*, *74*, 705–723. https://doi.org/10.1007/ s00445-011-0556-y

Sandri, L., Thouret, J.-C., Constantinescu, R., Biass, S., & Tonini, R. (2014). Long-term multi-hazard assessment for El Misti Volcano (Peru). *Bulletin of Volcanology*, *76*, 771. https://doi.org/10.1007/ s00445-013-0771-9

Santacroce, R., Cioni, R., Marianelli, P., Sbrana, A., Sulpizio, R., Zanchetta, G., et al. (2008). Age and whole rock-glass compositions of proximal pyroclastics from the major explosive eruptions of Somma-Vesuvius: A review as a tool for distal tephrostratigraphy. *Journal of Volcanology and Geothermal Research*, *177*(1), 1–18.

Selva, J. (2013). Long-term multi-risk assessment: Statistical treatment of interaction among risks. *Natural hazards*, *67*, 701–722.

Selva, J., Costa, A., Marzocchi, W., & Sandri, L. (2010). BET_VH: Exploring the influence of natural uncertainties on long-term hazard from tephra fallout at Campi Flegrei (Italy). *Bulletin of Volcanology*, *72*, 717–733. https://doi.org/10.1007/s00445-010-0358-7

Selva, J., Costa, A., Sandri, L., Macedonio, G., & Marzocchi, W. (2014). Probabilistic short-term volcanic hazard in phases of unrest: A case study for tephra fallout. *Journal of Geophysical Research: Solid Earth*, *119*, 8805–8826. https://doi.org/10.1002/2014JB011252

Selva, J., Orsi, G., Di Vito, M. A., Marzocchi, W., & Sandri, L. (2012). Probability hazard map for future vent opening at Campi Flegrei caldera, Italy. *Bulletin of Volcanology*, *74*, 497–510. https://doi.org/10.1007/ s00445-011-0528-2

Senior Seismic Hazard Analysis Committee (1997). Recommendations for probabilistic seismic hazard analysis-guidance on uncertainty and use of experts, U.S. Nuclear Regulatory Commission, NUREG/CR-6372.

Sevink, J., van Bergen, M. J., van der Plicht, J., Feiken, H., Anastasia, C., & Huizinga, A. (2011). Robust date for the Bronze Age Avellino eruption (Somma-Vesuvius): 3945 ±10 calBP (1995 ±10 calBC). *Quaternary Science Reviews*, *30*(9), 1035–1046.

Sheridan, M., & Malin, M. (1983). Application of computer-assisted mapping to volcanic hazard evaluation of surge eruptions: Vulcano, Lipari, and Vesuvius. *Journal of Volcanology and Geothermal Research*, *17*, 187–202. https://doi.org/10.1016/0377-0273(83)90067-7

Sheridan, M. F., Hubbard, B., Carrasco-Nunez, G., & Siebe, C. (2004). Pyroclastic flow hazard at Volcán Citlaltépetl. *Natural Hazards*, *33*(2), 209–221.

Smith, V., Isaia, R., & Pearce, N. (2011). Tephrostratigraphy and glass compositions of post-15 kyr Campi Flegrei eruptions: Implications for eruption history and chronostratigraphic markers. *Quaternary Science Reviews*, *30*(25), 3638–3660.

Spiller, E. T., Bayarri, M., Berger, J. O., Calder, E. S., Patra, A. K., Pitman, E. B., & Wolpert, R. L. (2014). Automating emulator construction for geophysical hazard maps. *SIAM/ASA Journal on Uncertainty Quantification*, *2*(1), 126–152.

Sulpizio, R., Mele, D., Dellino, P., & La Volpe, L. (2005). A complex, Subplinian-type eruption from low-viscosity, phonolitic to tephri-phonolitic magma: The AD 472 (Pollena) eruption of Somma-Vesuvius, Italy. *Bulletin of Volcanology*, *67*(8), 743–767.

Tadini, A., Bevilacqua, A., Neri, A., Cioni, R., Aspinall, W. P., Bisson, M., et al. (2017). Assessing future vent opening locations at the Somma-Vesuvio volcanic complex: 2. Probability maps of the caldera for a future Plinian/sub-Plinian event with uncertainty quantification. *Journal of Geophysical Research*, *122*, 4357–4376. https://doi.org/10.1002/2016JB013860

Tierz, P., Sandri, L., Costa, A., Sulpizio, R., Zaccarelli, L., Di Vito, M. A., & Marzocchi, W. (2016). Uncertainty assessment of Pyroclastic Density Currents at Mt Vesuvius (Italy) simulated through the Energy Cone Model. In P. Webley, K. Riley, & M. Thompson (Eds.), *Natural hazard uncertainty assessment: Modeling and decision support*. Washington, DC: American Geophysical Union.

Tierz, P., Sandri, L., Costa, A., Zaccarelli, L., Di Vito, M. A., Sulpizio, R., & Marzocchi, W. (2016). Suitability of energy cone for probabilistic volcanic hazard assessment: Validation tests at Somma-Vesuvius and Campi Flegrei (Italy). *Bulletin of Volcanology*, *78*, 79–92. https://doi.org/10.1007/s00445-016-1073-9

Todesco, M., Neri, A., Esposti Ongaro, T., Papale, P., Macedonio, G., Santacroce, R., & Longo, A. (2002). Pyroclastic flow hazard assessment at Vesuvius (Italy) by using numerical modeling. I. Large-scale dynamics. *Bulletin of Volcanology*, *64*(3-4), 155–177.

Tonini, R., Sandri, L., Costa, A., & Selva, J. (2015). Brief communication: The effect of submerged vents on probabilistic hazard assessment for tephra fallout. *Natural Hazards and Earth System Sciences*, *15*, 409–415. https://doi.org/10.5194/nhess-15-409-2015

Tonini, R., Sandri, L., & Thompson, M. A. (2015). PyBetVH: A Python tool for probabilistic volcanic hazard assessment and for generation of Bayesian hazard curves and maps. *Computer and Geosciences*, *79*, 38–46. https://doi.org/10.1016/j.cageo.2015.02.017

Valentine, G. (1998). Damage to structures by pyroclastic flows and surges, inferred from nuclear weapons effects. *Journal of Volcanology and Geothermal Research*, *87*(1), 117–140.

Wilson, L., Sparks, R., Huang, T., & Watkins, N. (1978). The control of volcanic column heights by eruption energetics and dynamics. *Journal of Geophysical Research*, *83*(B4), 1829–1836.